

Supercritical accretion disks with black holes

S.Fabrika (SAO)

Shakura-Sunyaev disks

Astron. & Astrophys. 24, 337–355 (1973)

Black Holes in Binary Systems. Observational Appearance

N. I. Shakura

Sternberg Astronomical Institute, Moscow, U.S.S.R.

R. A. Sunyaev

Institute of Applied Mathematics, Academy of Sciences, Moscow, U.S.S.R.

Received June 6, 1972

thin = α -disks = standard = radiative

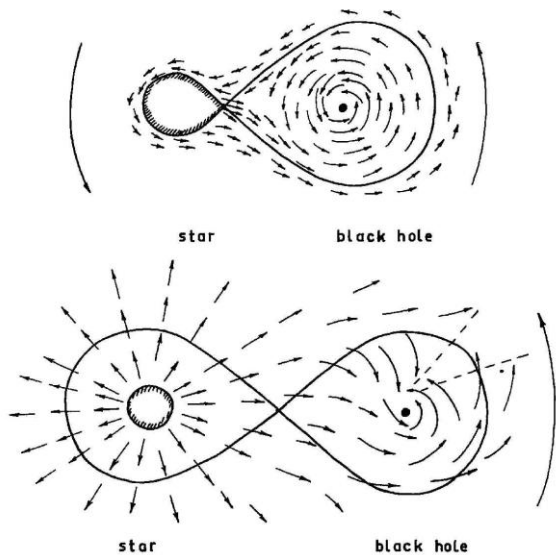


Fig. 1. Two regimes of matter capture by a collapsar: a) a normal companion fills up its Roche lobe, and the outflow goes, in the main, through the inner lagrangian point; b) the companion's size is much less than Roche lobe the outflow is connected with a stellar wind. The matter loses part of its kinetic energy in the shock wave and thereafter, gravitational capture of accreting matter becomes possible

matter enable angular momentum to be transferred outward. The efficiency of the mechanism of angular momentum transport is characterized by parameter $\alpha = \frac{v_t}{v_s} + \frac{H^2}{4\pi\varrho v_s^2}$ where $\frac{\varrho v_s^2}{2} = \frac{3}{2}\varrho \frac{kT}{m_p} + \varepsilon_r$ is the thermal energy density of the matter, ε_r is the energy density of the radiation, v_s is the sound velocity and v_t the turbulent velocity. In part II below we show that $\alpha \leq 1$. The most probable model is that of accretion with formation of a disk around the black hole (Prendergast, 1960; Gorbatsky, 1965; Burbidge and Prendergast, 1968; Lynden-Bell, 1969; Shakura, 1972; Pringle and Rees, 1972). The particles in the disk, due to friction between adjacent layers, lose their angular momentum and spiral into the black hole²). Gravitational energy is released during this spiraling. Part of this energy increases the kinetic energy of rotation and the other part turns into the thermal energy and is radiated from the disk surface. The total energy release and the spectrum of the outgoing radiation are determined mainly by the rate of accretion, i.e. by the rate inflow

SS73 disk:

$$H/R \sim c_s/v_k$$

thin

$$v_r \sim \alpha v_k (H/R)^2$$

slow

$$T \text{ propto } r^{-3/4}$$

multitemperarure

$$T_{in} \text{ propto } M^{-1/4}$$

$$L = \frac{GM_x \dot{M}_a}{R} \quad \text{- disk luminosity}$$

$$L = \eta \dot{M} c^2, \quad \eta = 0.06, \quad \eta \leq 0.42$$

Eddington limit:

$$L_E = \frac{4\pi GM_x c}{\kappa} \sim 1.5 \cdot 10^{38} m \text{ erg/s} \quad \text{- critical luminosity}$$

$$\begin{aligned} \dot{M}_{Edd} &= \frac{48\pi GM}{c\kappa} = 2 \cdot 10^{18} m \text{ g/s} \\ &= 3 \cdot 10^{-8} m M_{SUN} / y \end{aligned}$$

Restrictions in SS73

$$q_+ = q_- + q_{\text{adv}}; \quad q_{\text{adv}} = 0$$

Keplerian rotation heats protons via viscosity

Protons have (to have a time) to exchange the energy with electrons

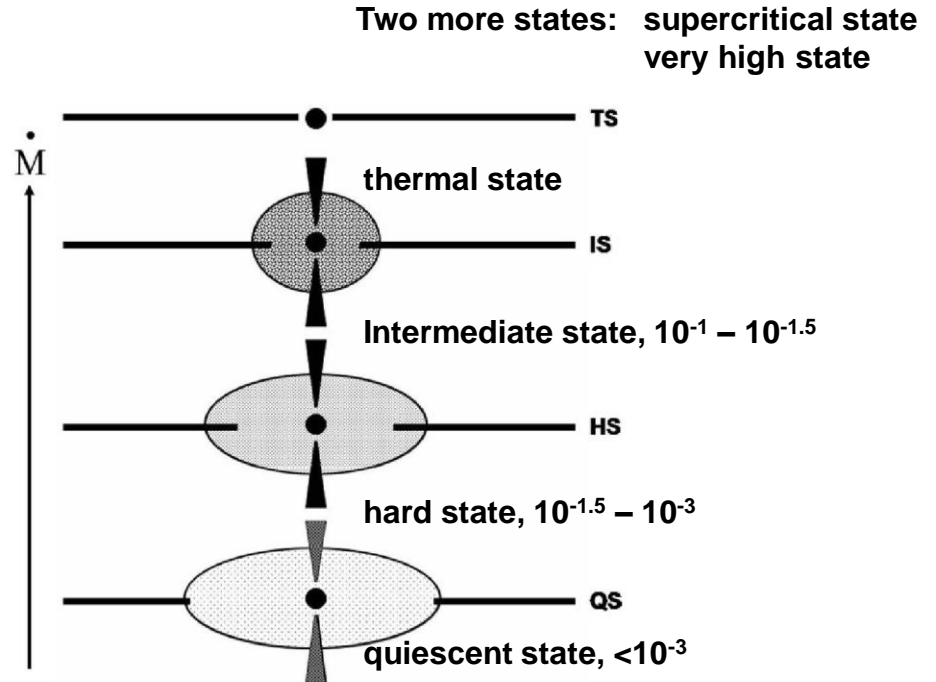
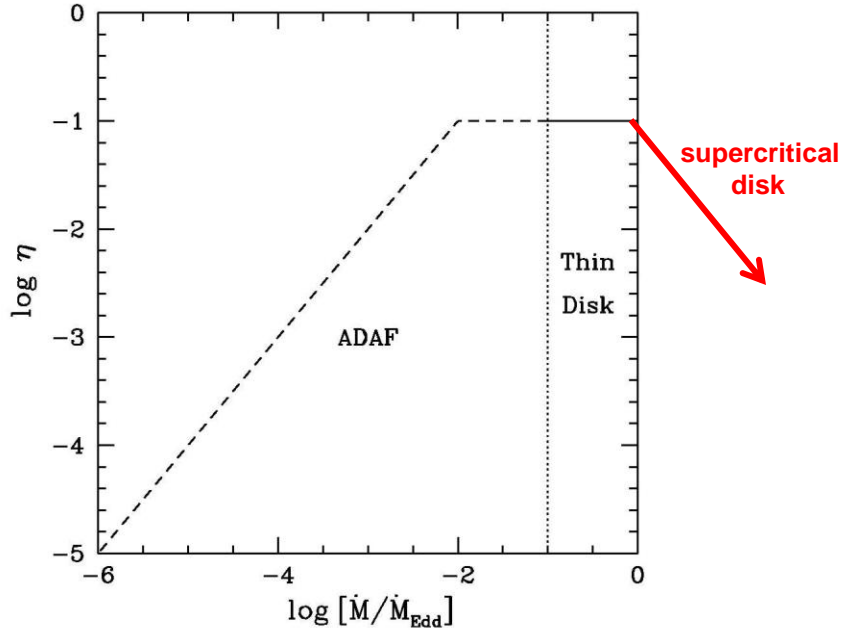
$$t_{\text{coll}} \ll t_{\text{accr}}, \quad \dot{m} > 0.01$$

Electrons loss the energy in radiation

The radiation has (to have a time) to escape the disk

$$t_{\text{diff}} \ll t_{\text{accr}}, \quad \dot{m} < 1-10$$

$$\dot{m} = \dot{M} / \dot{M}_{\text{Edd}}$$



Efficiency of accretion

$$\eta = L / \dot{M}c^2$$

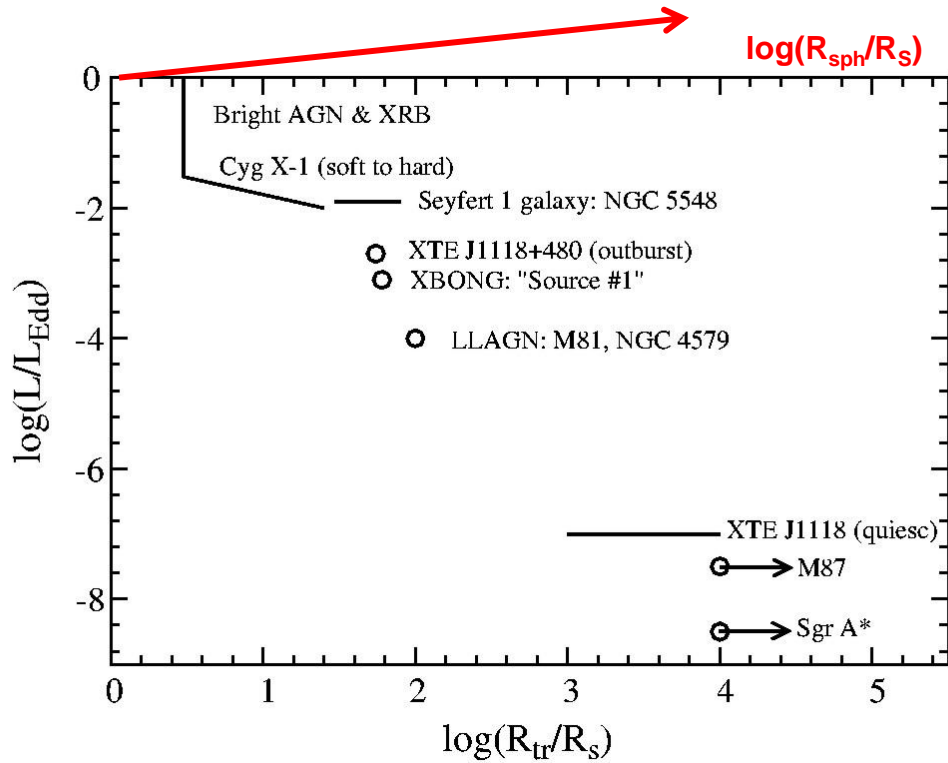
$$\text{at } \dot{m} = \frac{\dot{M}}{\dot{M}_{Edd}} > 1 \quad \eta \sim \dot{m}^{-1}$$

Narayan, McClintock (2008); Esin et al., (1997)

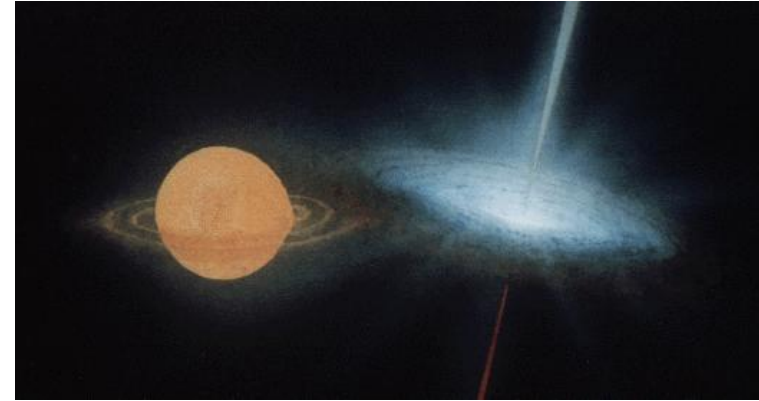
Microquasars and quasars

Why the jets launch?

When depart from the SS73's regime



Narayan, McClintock (2008)



3 models of supercritical disks:

Shakura-Sunyaev disk (1973). Strong wind outflow inside the spherization radius.

Slim-disk (Jaroszynski et al., 1980; Abramowicz et al., 1988; Watarai et al., 2000 ++). Account for advection of heat and radiation.

Computer RHD simulations (Eggum, Coroniti, Kats, 1988; Okuda et al., 1997-2009; Ohsuga et al., 2005-2007).

Supercritical disk by Shakura-Sunyaev (1973):

$$R_{sph} \approx \frac{GM_x \dot{M}_a}{L_E} - \text{spherization radius}$$

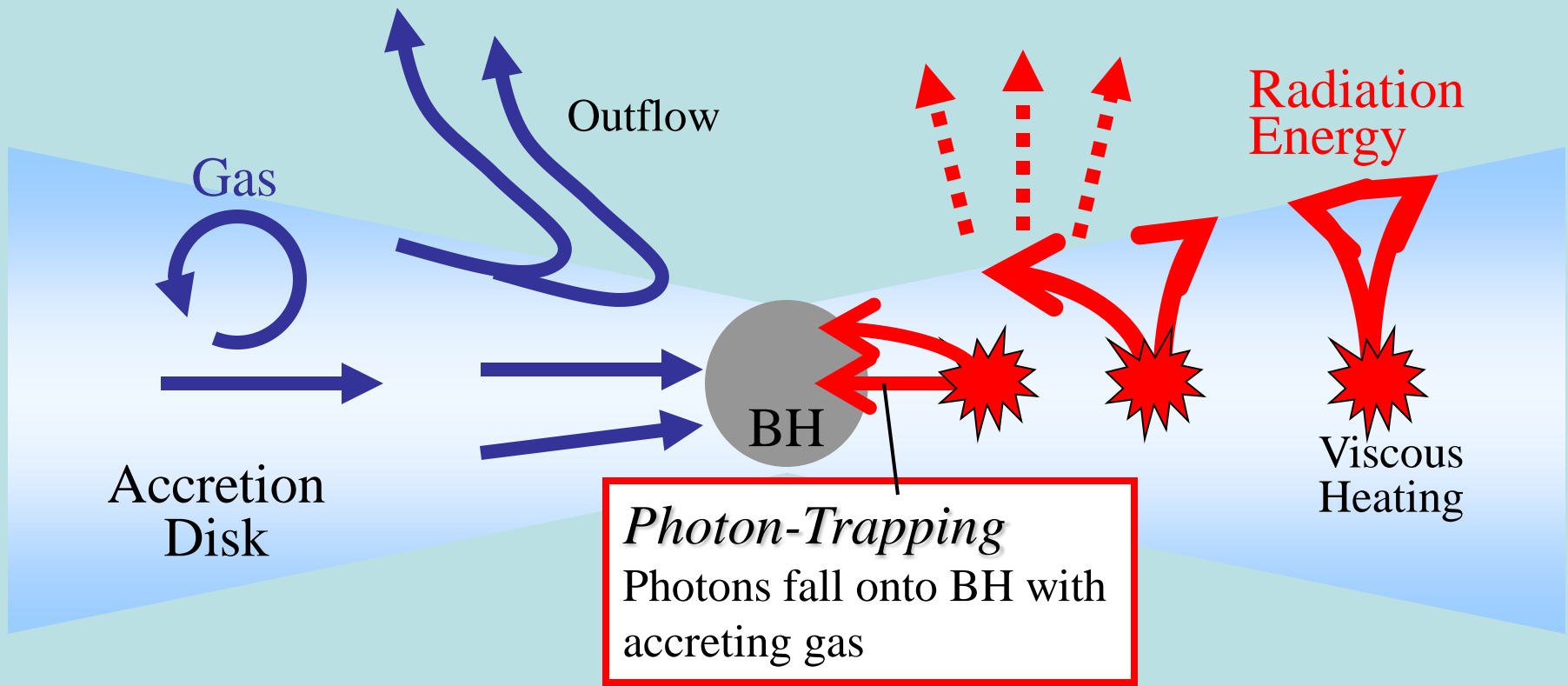
$$V_W \sim \left(\frac{2GM_x}{R_{sph}} \right)^{\frac{1}{2}} - \text{the disk wind velocity}$$

$$\dot{M}_W = \dot{M}_a - \dot{M}_E - \text{the mass loss rate}$$

Advection (inner disk overheating):

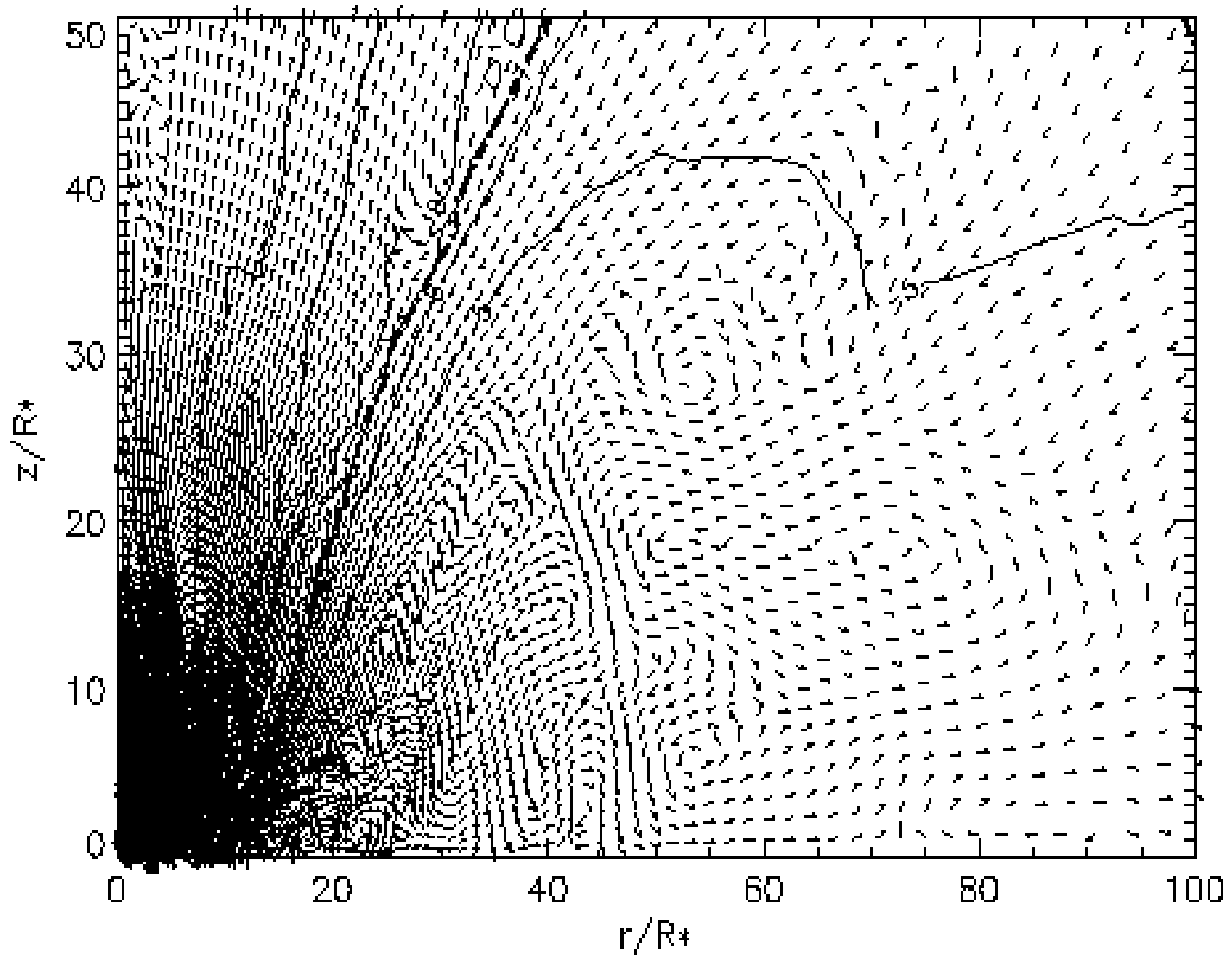
$$\dot{M}_W \sim 0.5 \dot{M}_a$$

Ohsuga et al (2005): the super-Eddington disk accretion flows, the 2D Radiation Hydrodynamic simulations.



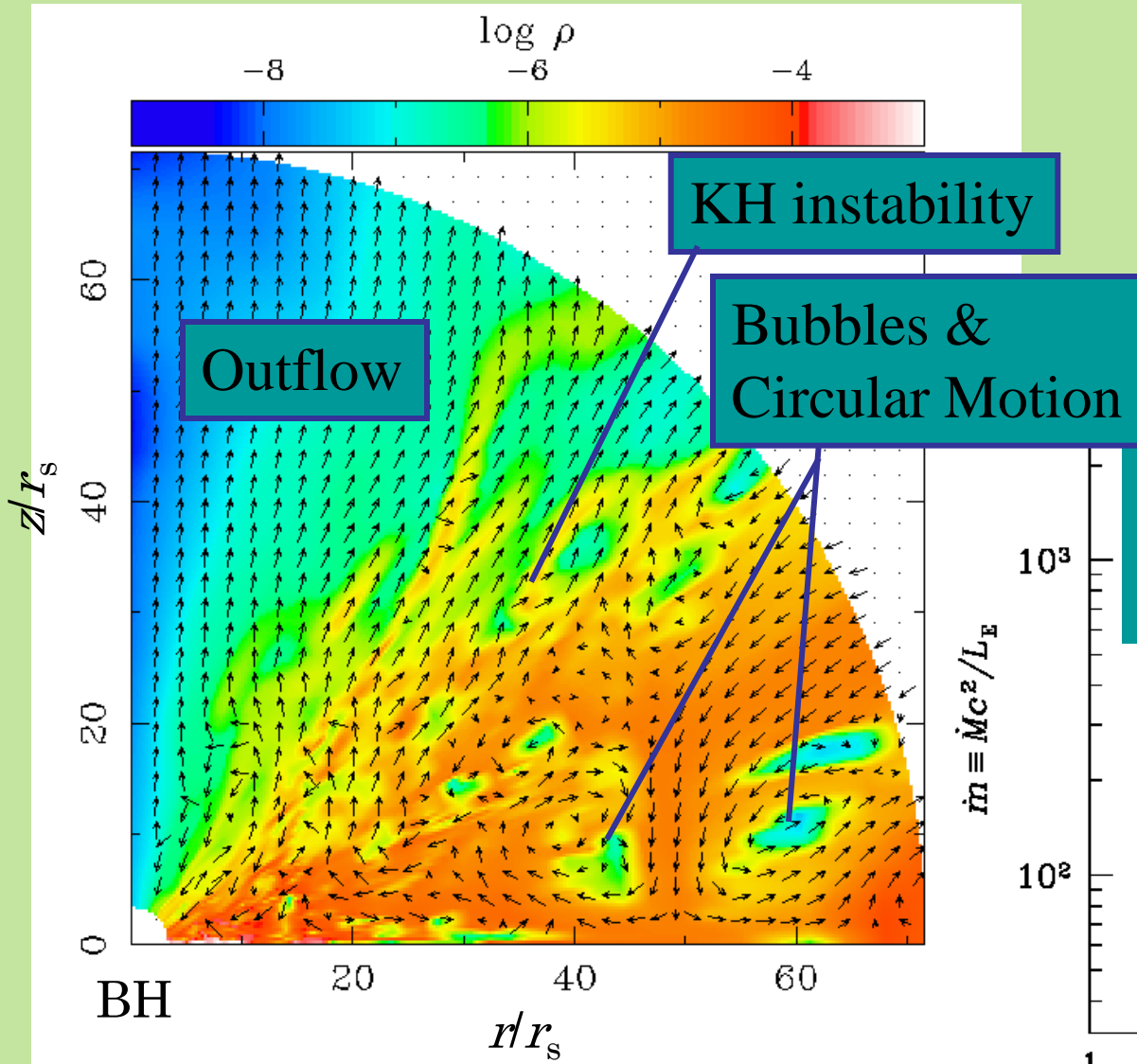
2D HD simulations with radiation

(Okuda, 2002)



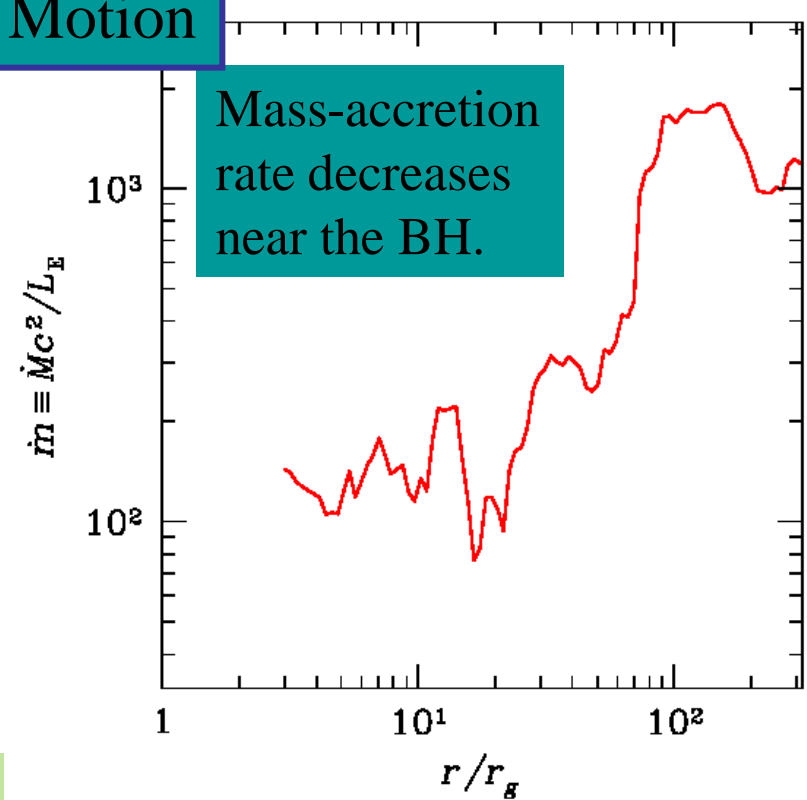
Quasi-steady Structure

Density & Velocity fields



Ohsuga et al. 2005,
ApJ, 628, 368

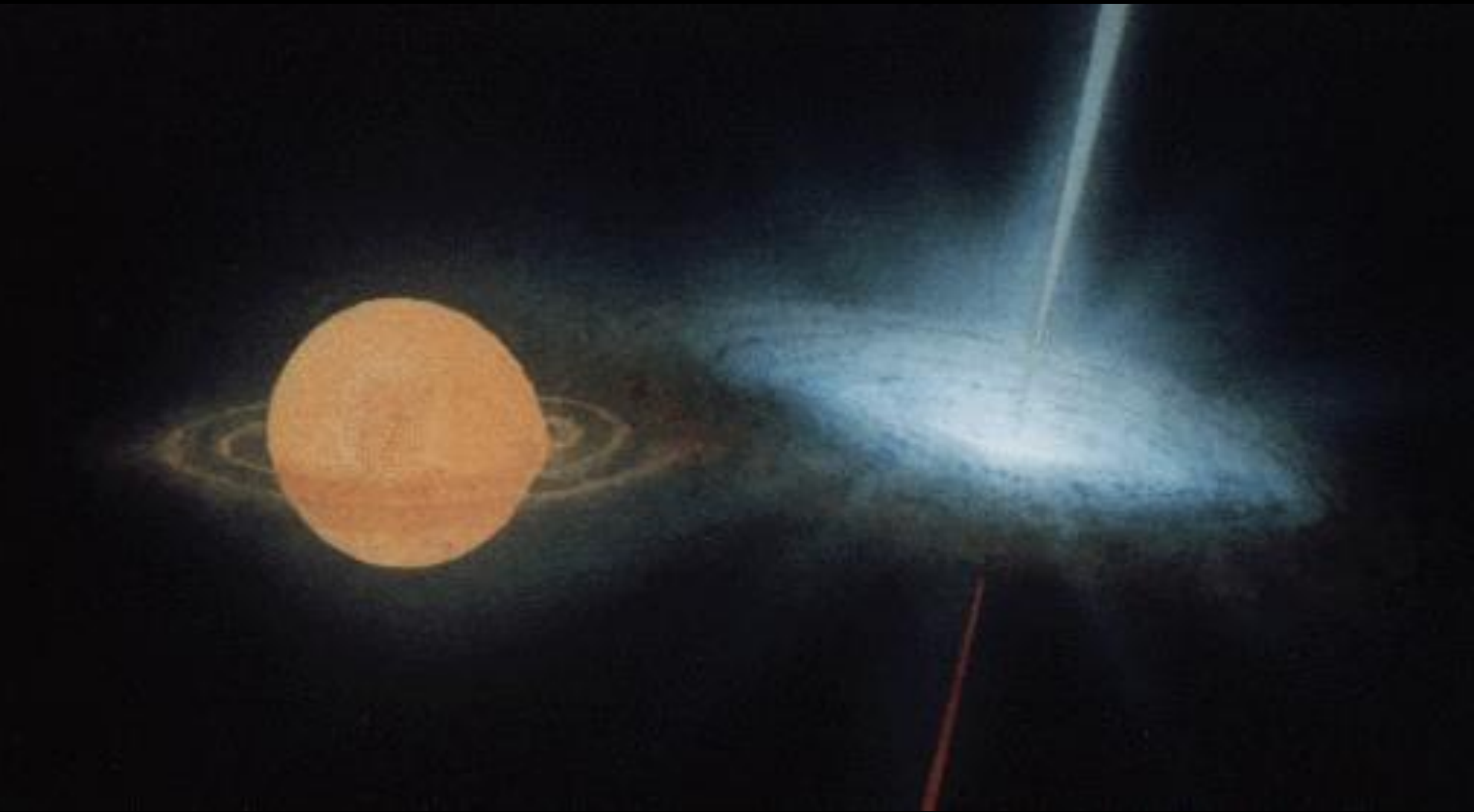
Mass-Accretion Rate



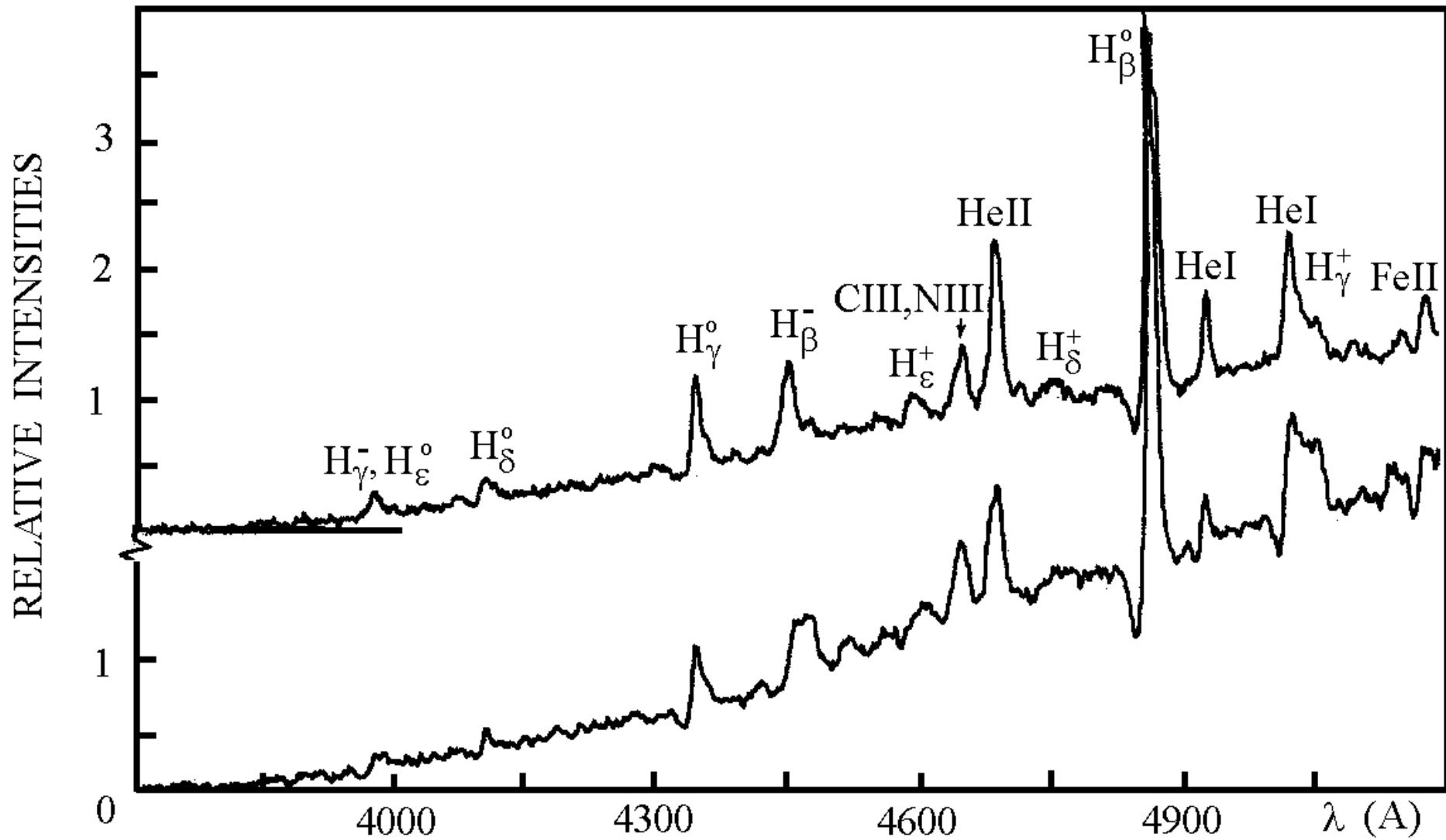
Objects:

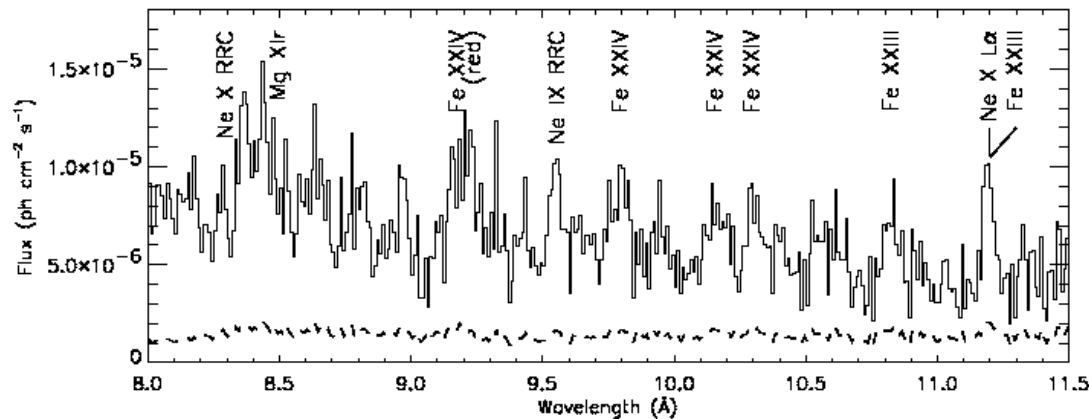
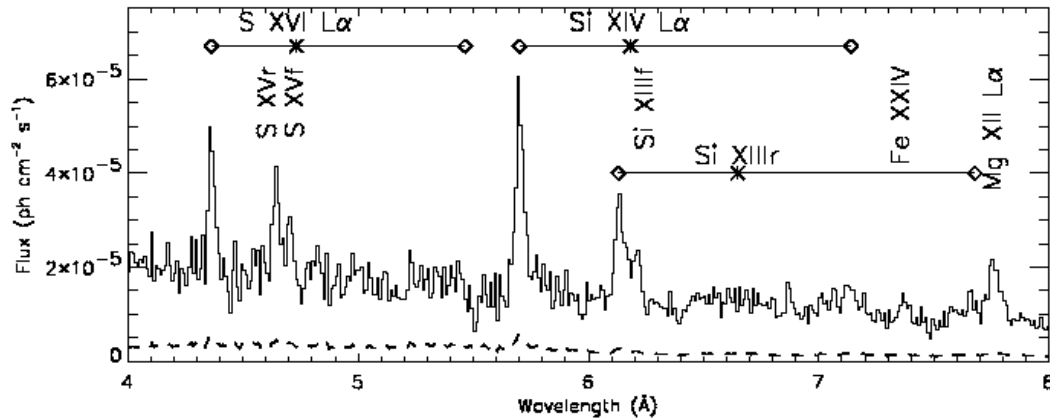
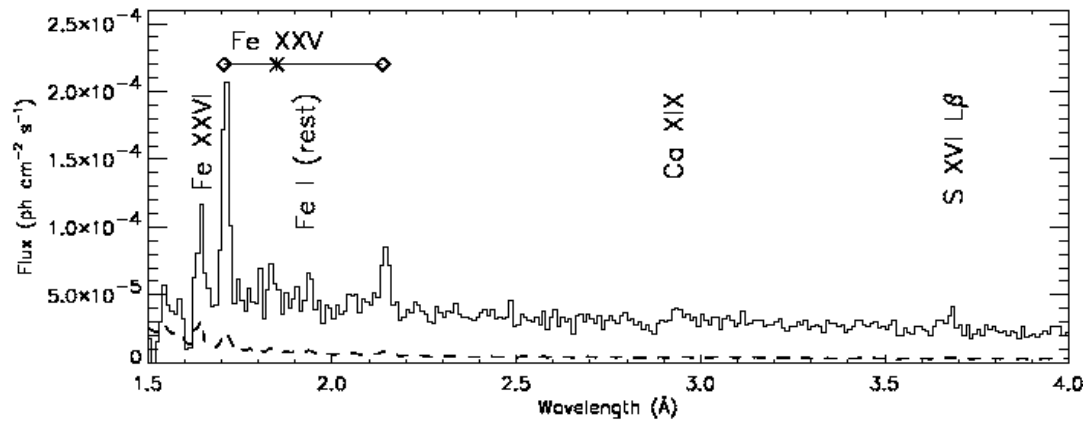
1. The close binary SS433 $\sim 10 M_{\text{SUN}}$
2. Ultraluminous X-ray sources (ULXs) in external galaxies $\sim 10 - 100 M_{\text{SUN}}$
3. Supermassive black holes in distant galaxies $10^5 - 10^{10} M_{\text{SUN}}$

SS433



SS433





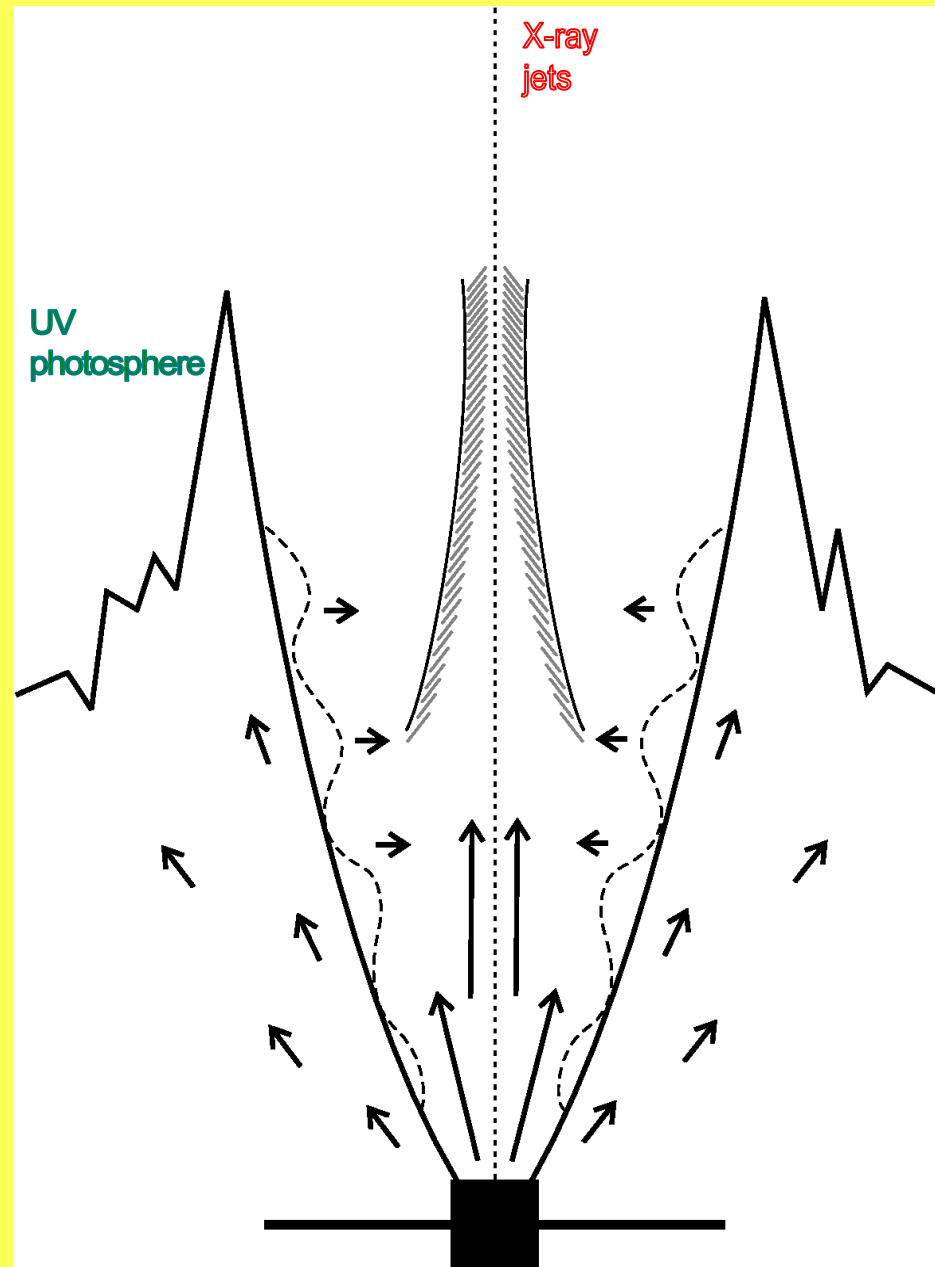
X-ray spectroscopy

SS433 from CHANDRA
Marshall et al. 2002

All the X-ray radiation is formed in the jets

The central X-ray machine is totally hidden

The supercritical disk and its funnel in SS433



$$\dot{M}_{wind} \sim 10^{-4} M_{\odot}/y$$

$$T_{wind} \sim (5-7) 10^4 K$$

$$V_{wind} \sim 1500 \text{ km/s}$$

$$L_{bol} \sim 10^{40} \text{ erg/s}$$

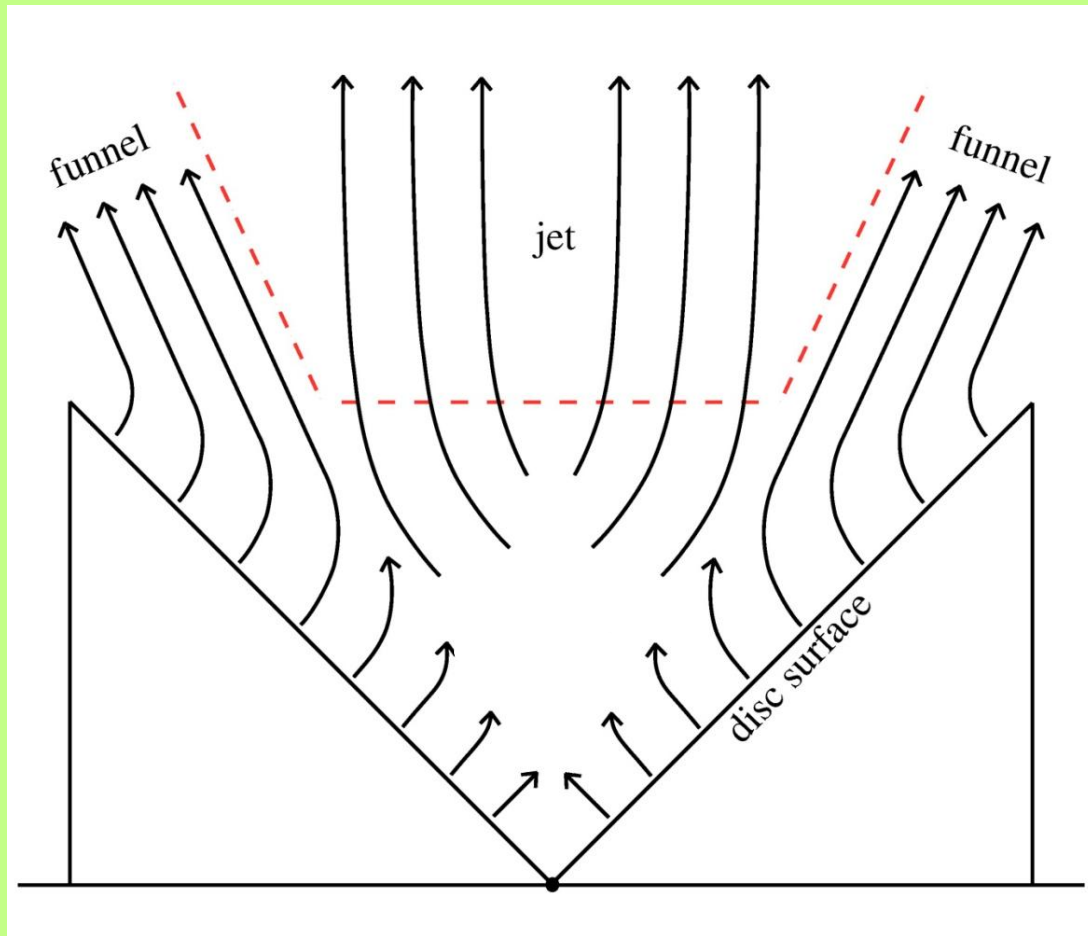
$$L_X \sim 10^{36} \text{ erg/s}$$

$$\text{Jets: } L_k \sim 10^{39} \text{ erg/s}$$

$$2 \theta_j \sim 1.5^\circ$$

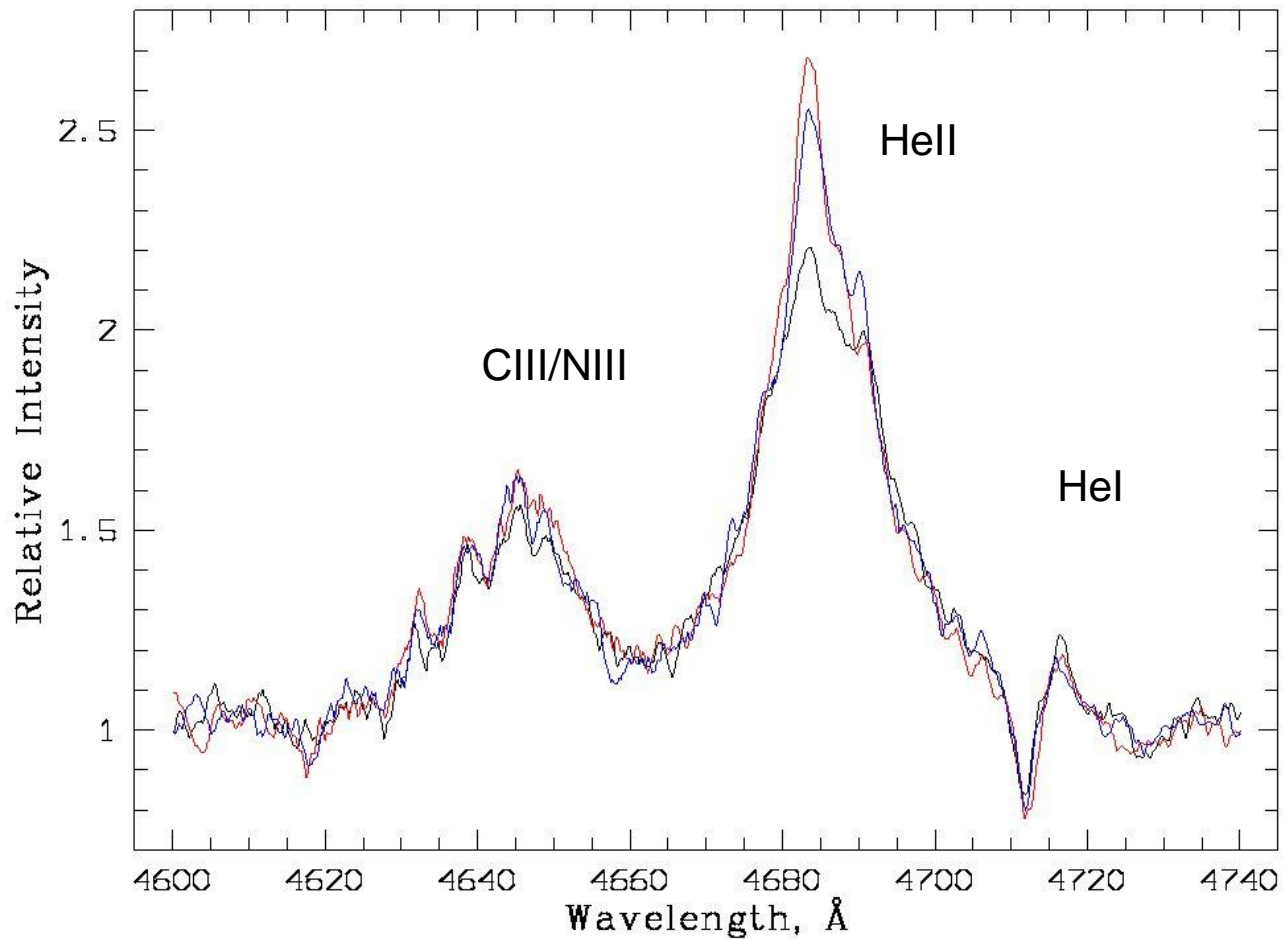
$$\text{Funnel: } 2 \theta_f \sim 50^\circ$$

Intrinsic X-ray budget of 10^{40} erg/s



Shakura-Sunyaev supercritical disk

HeII 4686 Å emission line formed in the supercritical disk wind



WHT spectra of SS433. 30 min variability

Spectral energy distribution of SS433 as seen edge-on and face-on

SS433 is ultraluminous

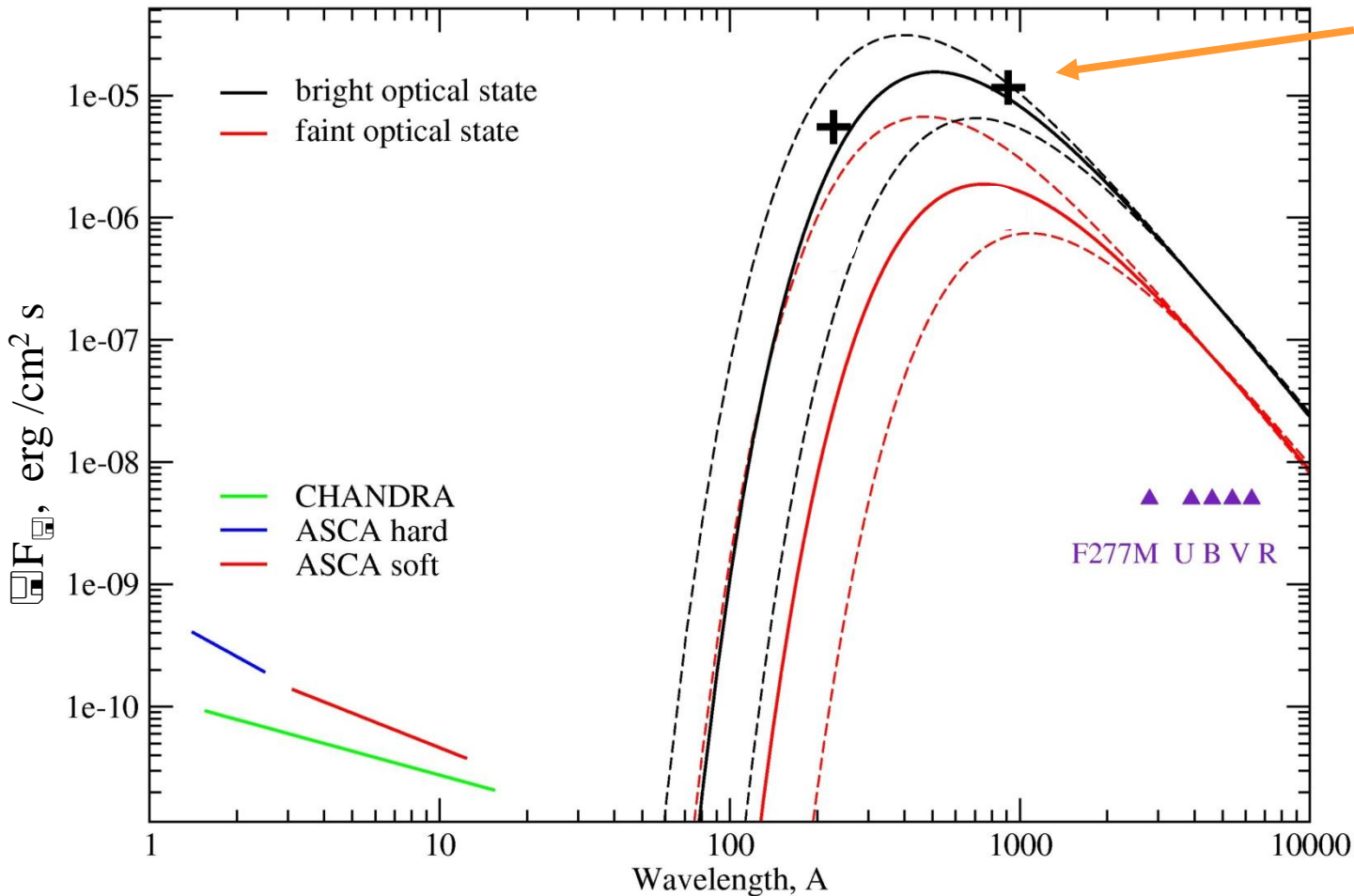


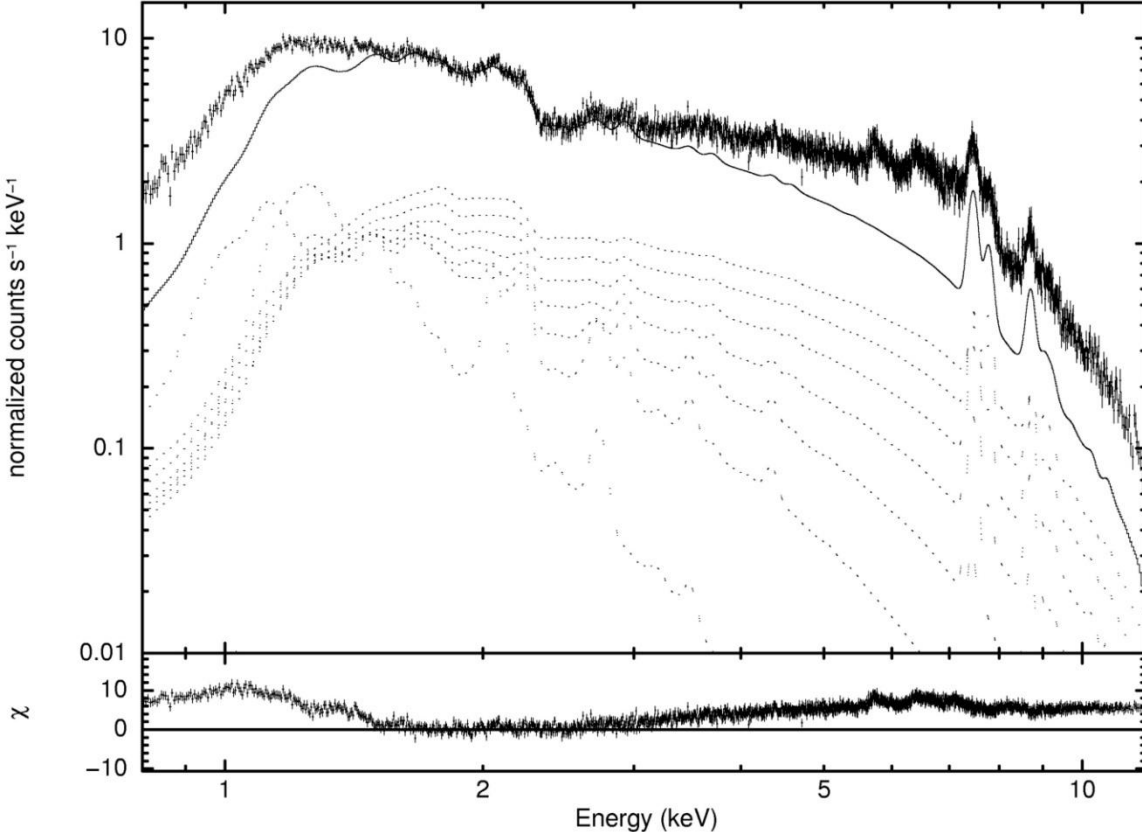
Face-on Zanstra estimates
Fabrika, Sholukhova, 2008

Nearly isotropical
ultraluminous UV
source $\sim 10^{40}$ erg/s,
 $T \sim 10^5$ K

HST and ground-base
spectral fit ($A_V \sim 8.0$)
Dolan et al. 1997

X-rays:
Kotani et al. 1996
Marshall et al. 2002





XMM-Newton observes SS433

Thermal jets + reflection
in the X-ray spectra

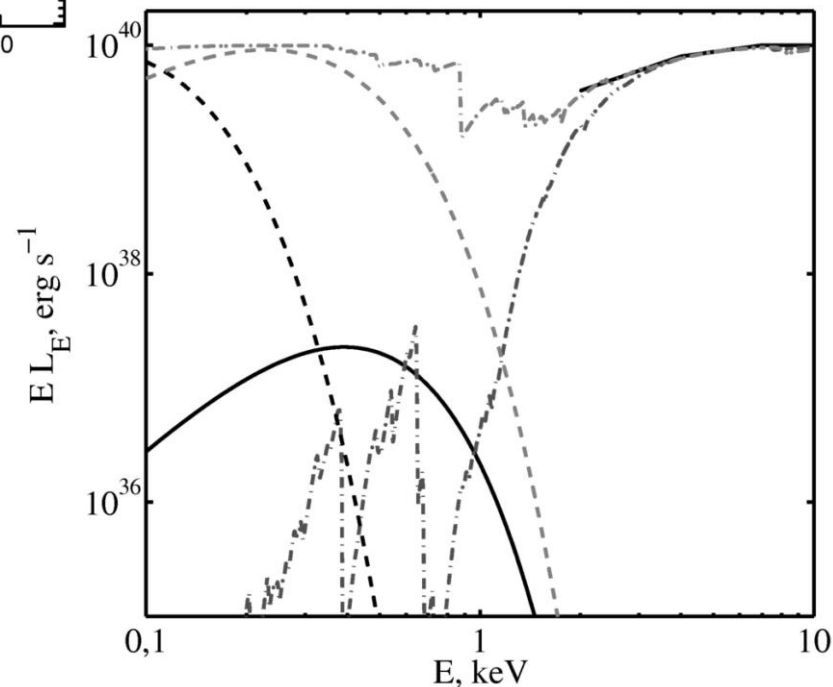
Medvedev, Fabrika (2009)

Multitemperatute relativistic jets
+ partly ionized reflection
+ BB or MCF spectrum of outer funnel walls

The illuminating spectrum is flat
($E F_E \sim E^0$) and strongly absorbed

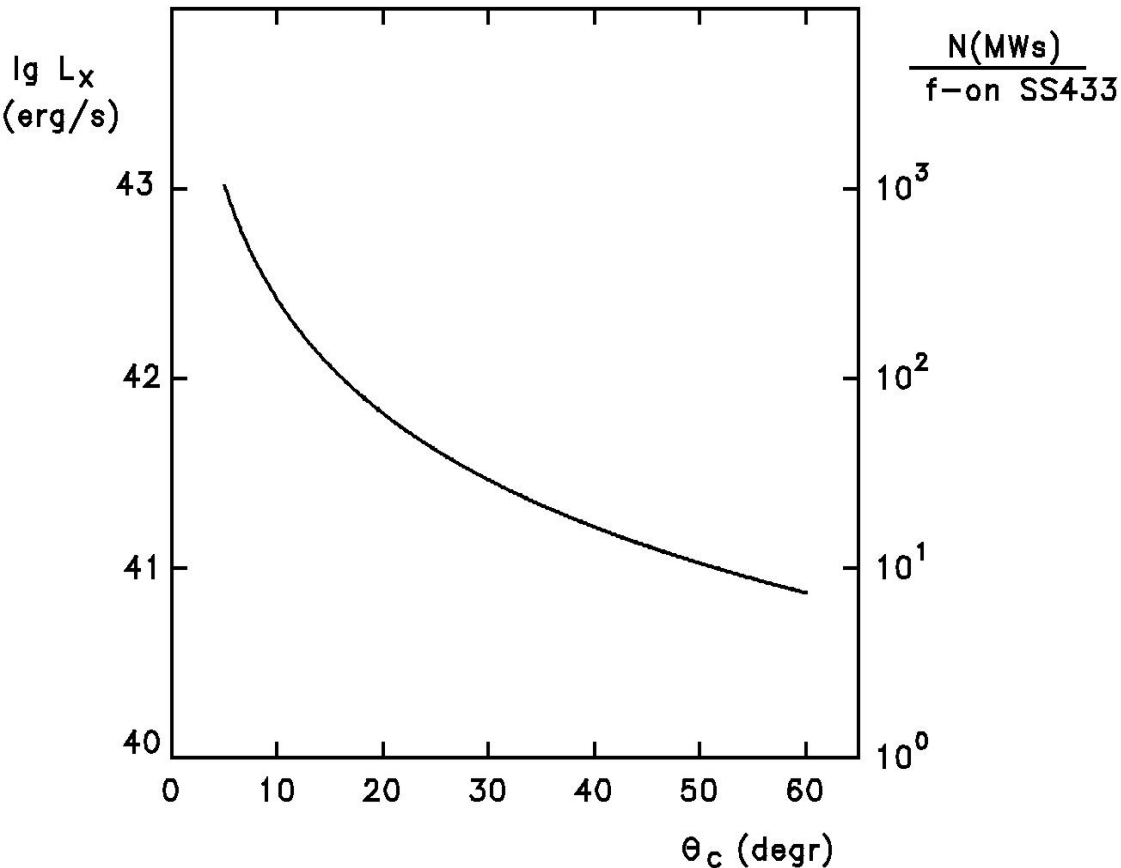
The soft X-ray excess. The same as in ULXs

Nickel excess in the jets (x 8-10)



SS433 disk observed face-on

Fabrika, Mescheryakov (2001)



$$L_{\text{Edd}}(10M_{\odot}) \sim 10^{39} \text{ erg/s}$$

$$\times \left(1 + \ln \left(\frac{\dot{M}}{\dot{M}_{\text{Edd}}} \right) \right) \sim 7$$

$$\times \Omega_f / 2\pi \sim 10$$

$$\Rightarrow L_{\text{x,obs}} \sim 10^{41} \text{ erg/s}$$

The observed luminosity of SS433:

$$L_{\text{bol}} \sim 10^{40} \text{ erg/s}, \quad \text{adopt } L_{\text{funnel}} \sim L_{\text{bol}}$$

Ultraluminous X-ray sources (ULXs)

X-ray luminosities $L_{0.5-100 \text{ keV}} \sim 10^{39-42} \text{ erg/s}$

X-ray luminosities of stellar mass black holes and galaxies:

Luminosity of “ordinary” black hole in a close binary

$$L_x \sim 10^{37} \text{ erg/s}$$

Critical luminosity of a black hole (10 solar masses)

$$L_x \sim 10^{39} \text{ erg/s}$$

X-ray luminosity of “an ordinary” galaxy

$$L_x \sim 10^{40} \text{ erg/s}$$

ULX in peculiar SN remnant MF16 in NGC6946



X-1 $L_x \sim 3 \cdot 10^{39}$ erg/s

CARTWHEEL GALAXY



$L_x \sim 10^{41}$ erg/s



CHANDRA X-RAY



GALEX ULTRAVIOLET

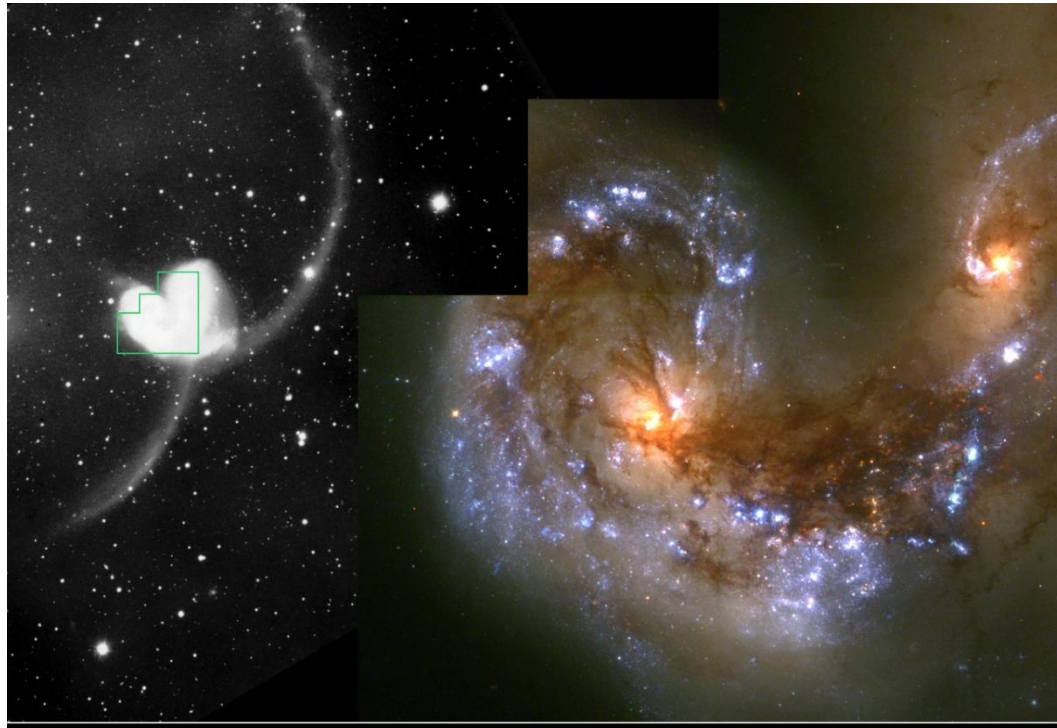


HUBBLE VISIBLE

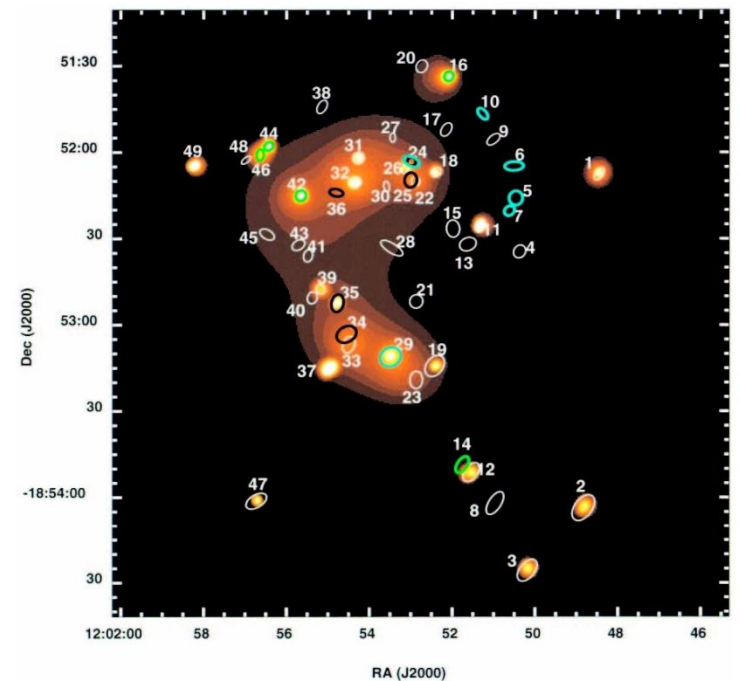
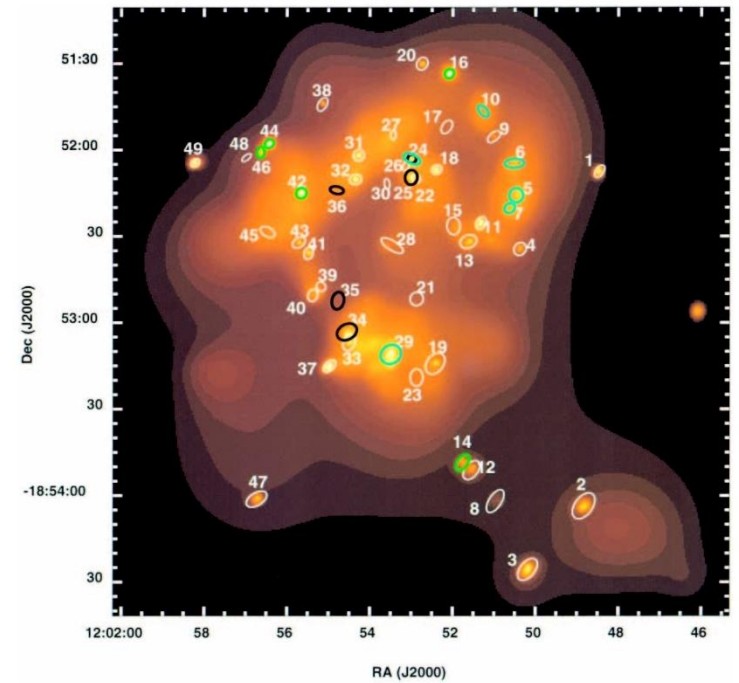


SPITZER INFRARED

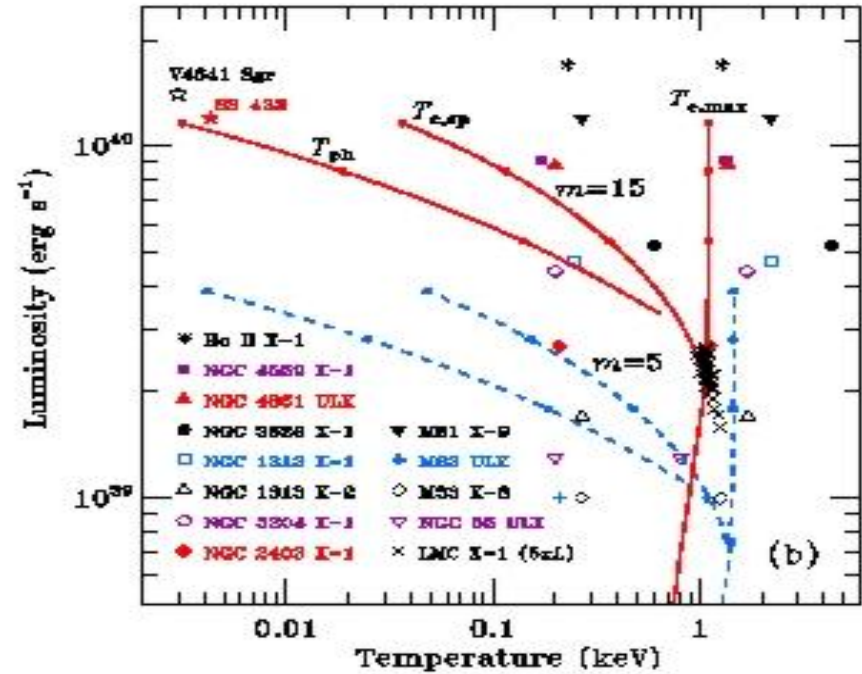
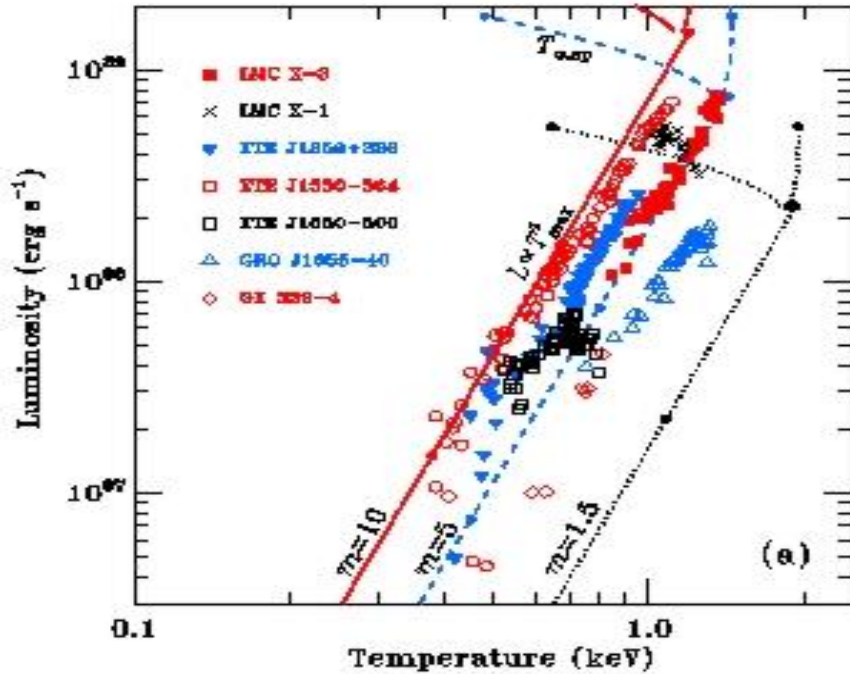
ULXs in Antennae Chandra (Zezas et al., 2002)



Colliding Galaxies NGC 4038 and NGC 4039
Hubble Space Telescope • Wide Field Planetary Camera 2



Temperatures of ULXs and galactic black holes (Poutanen et al., 2007)



The supercritical disks must produce flat X-ray spectra

$$EF_E \propto E^{-\alpha}, \quad \alpha \sim 0$$

The disks are supported by radiation

$$Q \propto r^{-2} \propto \sigma T^4, \quad T \propto r^{-1/2}$$

Models of ULXs

1. Supercritical disks in close binaries with a black hole (like SS433) observed nearly face-on.

Geometrical collimation

2. Intermediate mass black holes (IMBHs) $\sim 10^2 - 10^4 M_{\odot}$.
To produce ULXs the IMBHs must be in close binaries with massive donors.

Extention of Eddington limit

Optical Spectroscopy:

All ULXs studied have strong, broad (~ 1000 km/s) and variable HeII 4686 Å emission, weak and broad hydrogen lines.

1) WN-type donor?

Can not provide observed X-ray luminosity.

2) IMBHs, the HeII emission arises in accretion disk heated by the BH?

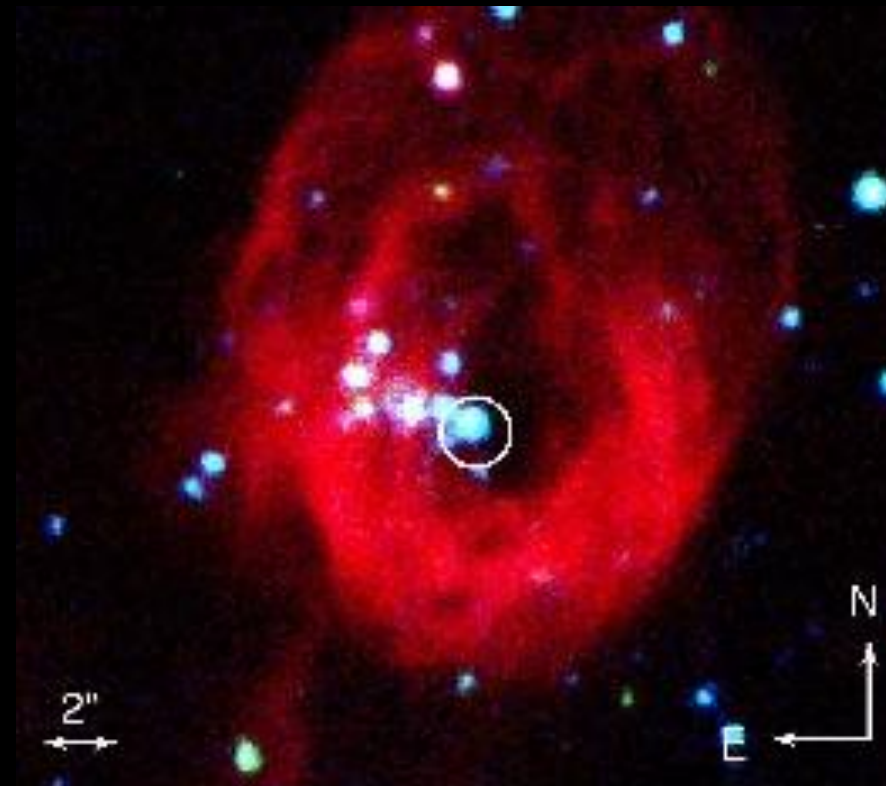
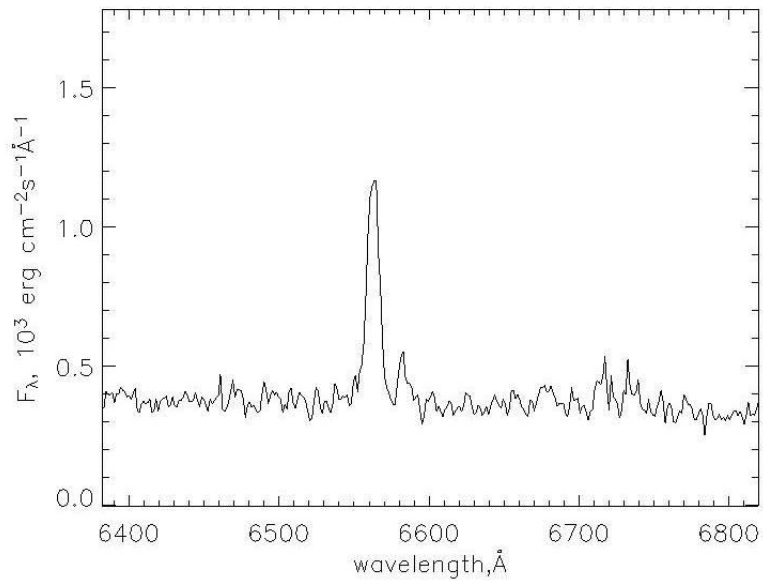
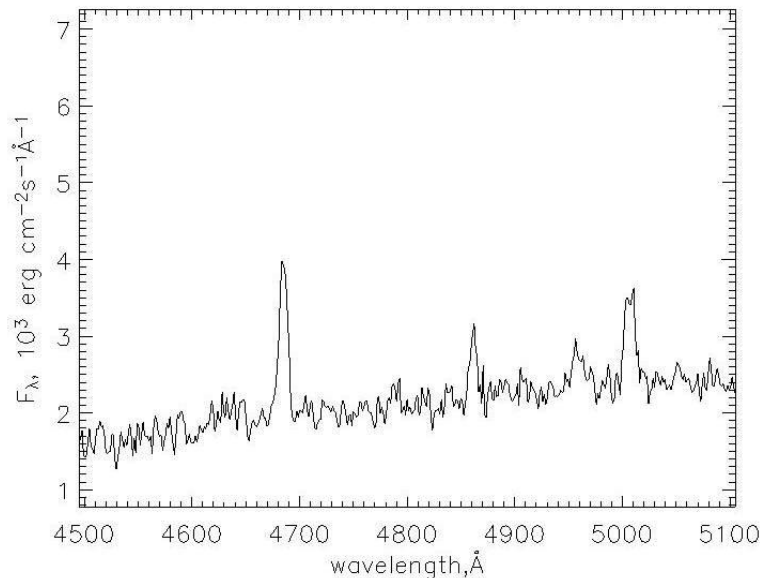
Optical and UV luminosities are too high for a standard disk.

Why the strong variability?

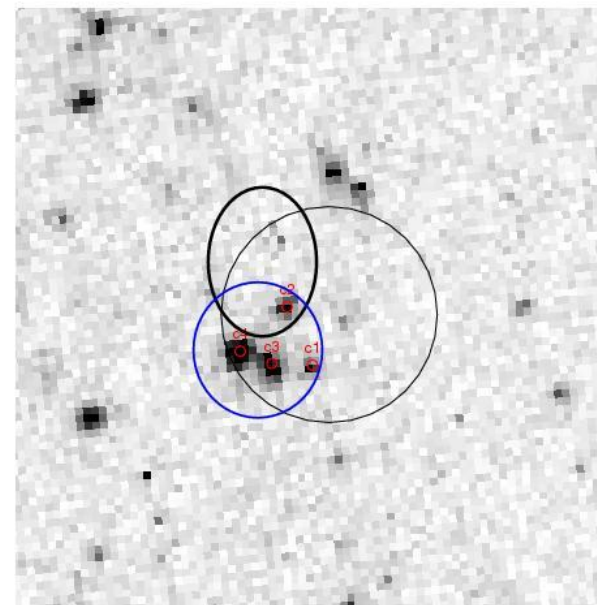
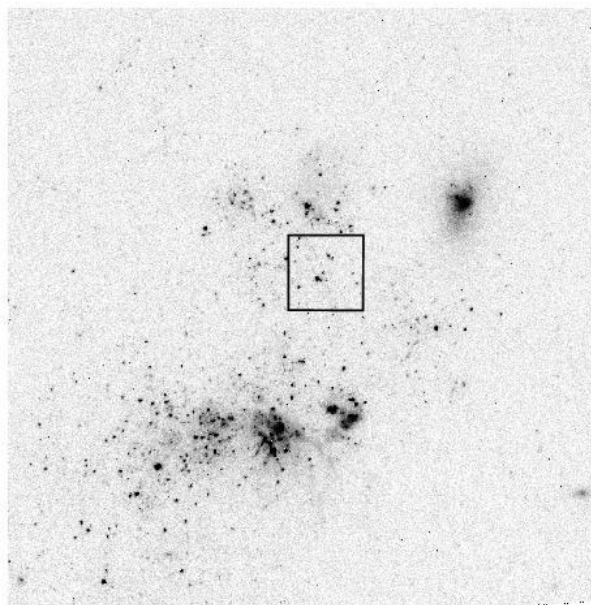
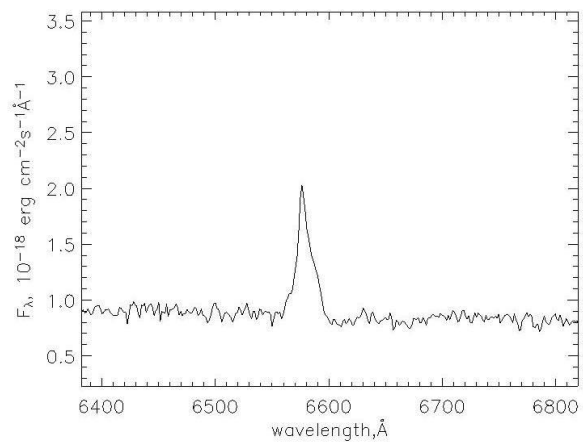
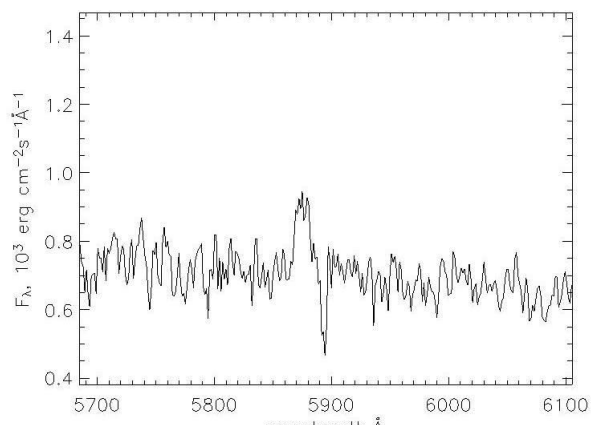
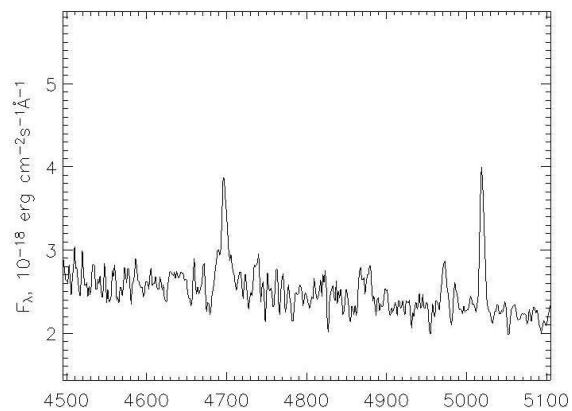
3) Supercritical disks like that in SS433?

4) New type of X-ray sources?

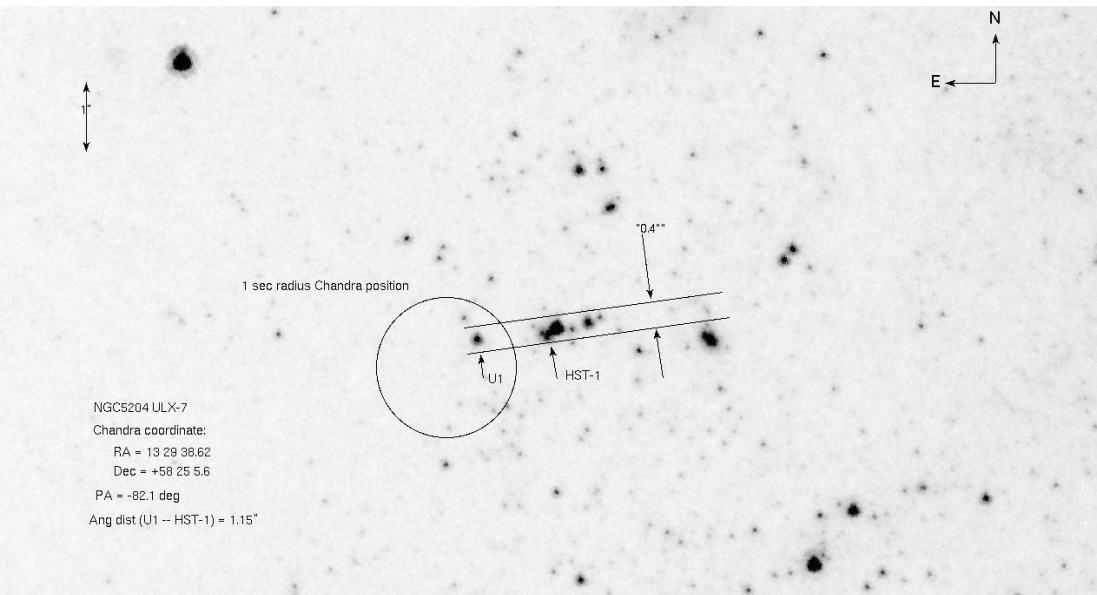
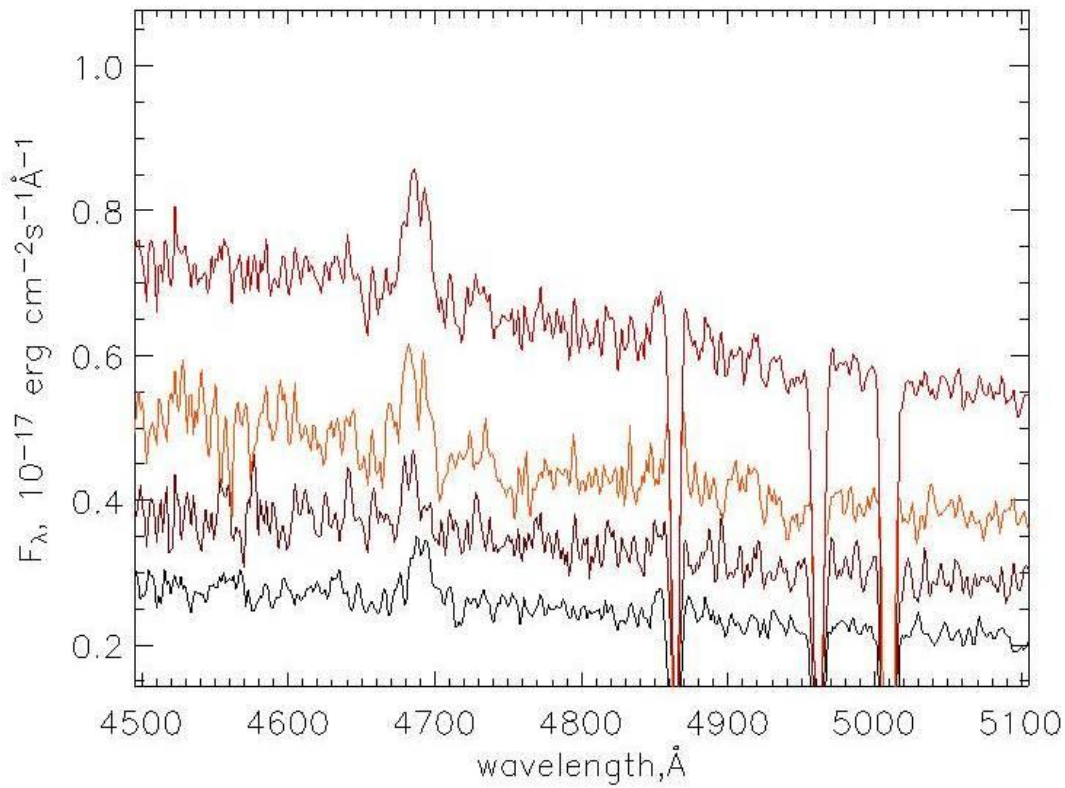
Holmberg IX X-1 (3.6 Mpc)



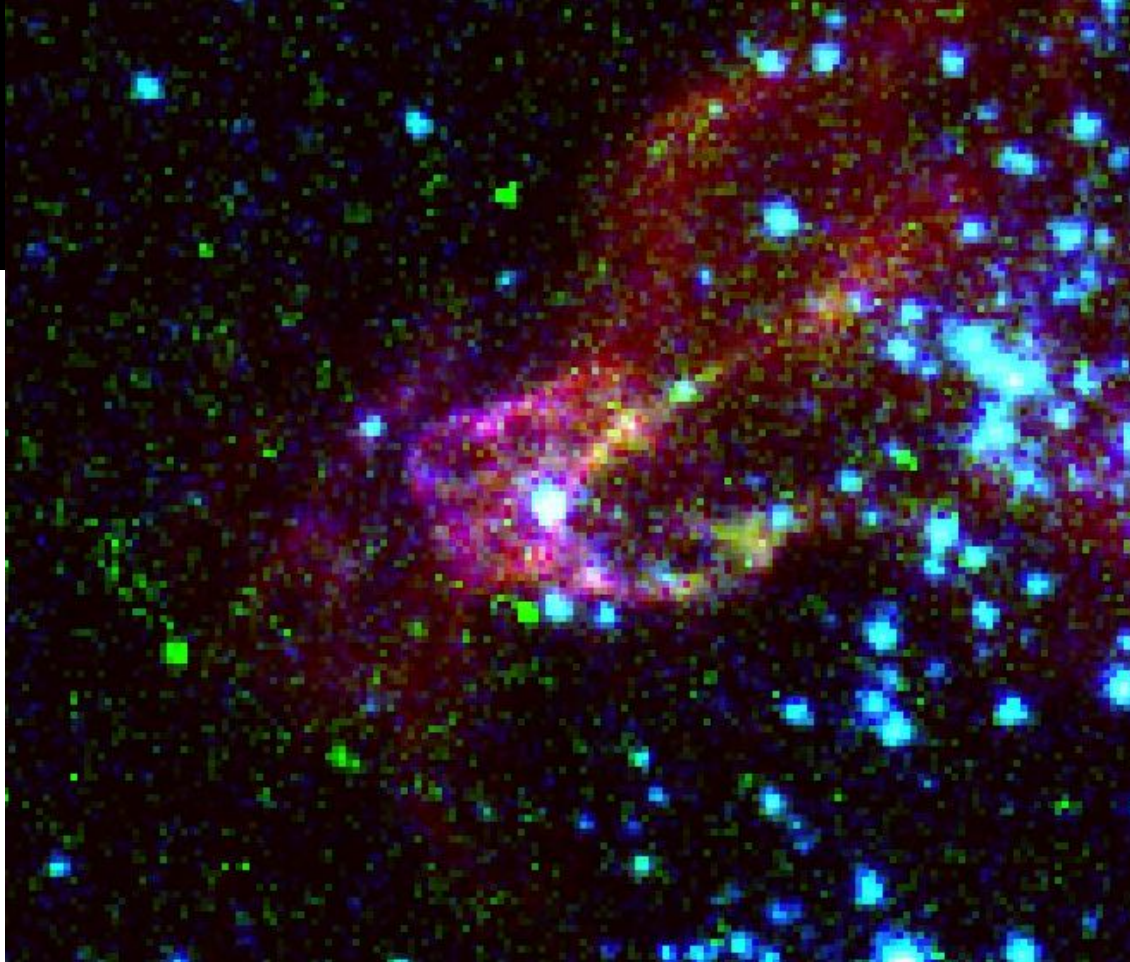
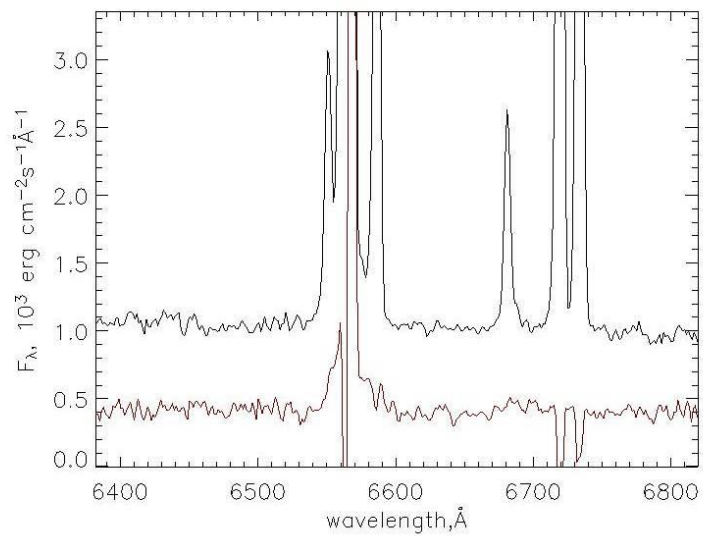
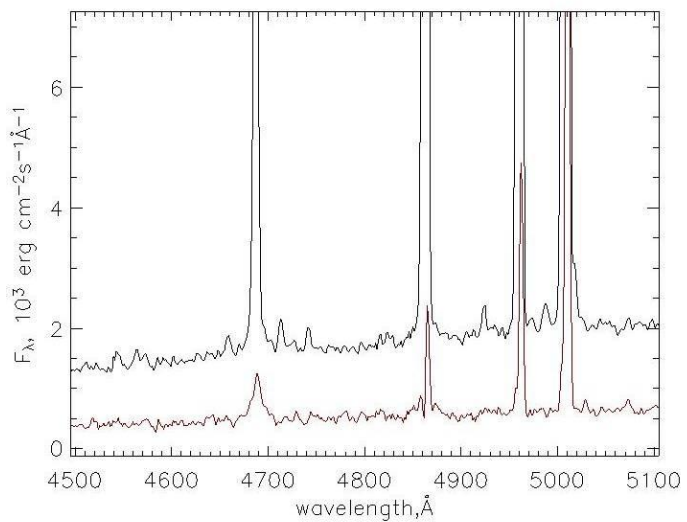
NGC 4559 X-1 (10.0 Mpc)

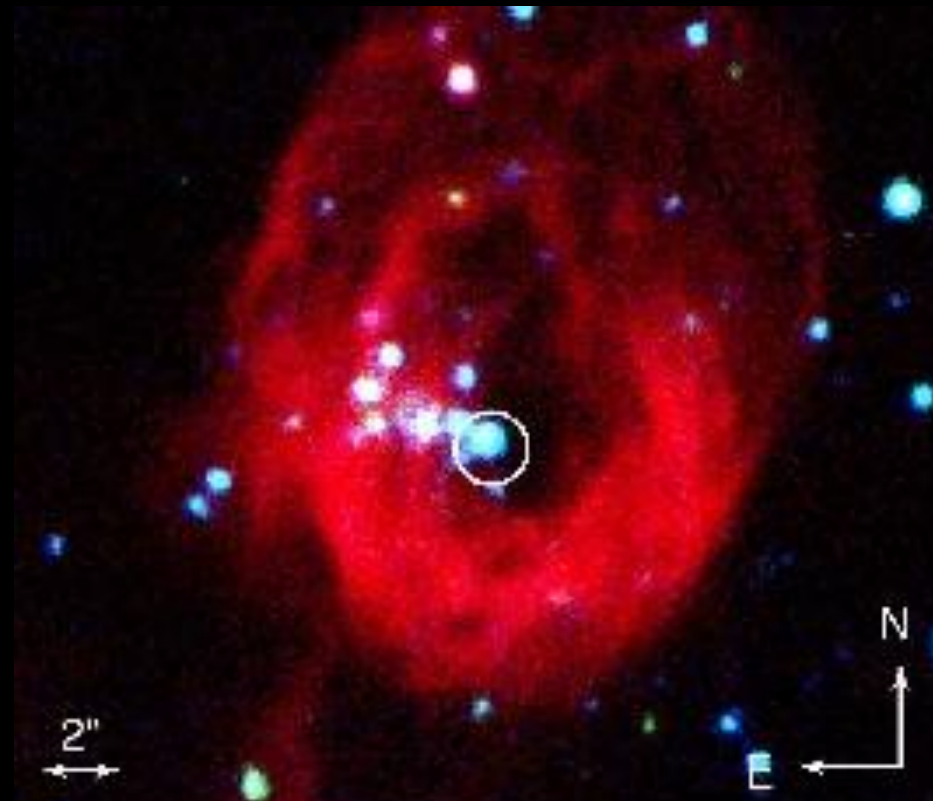
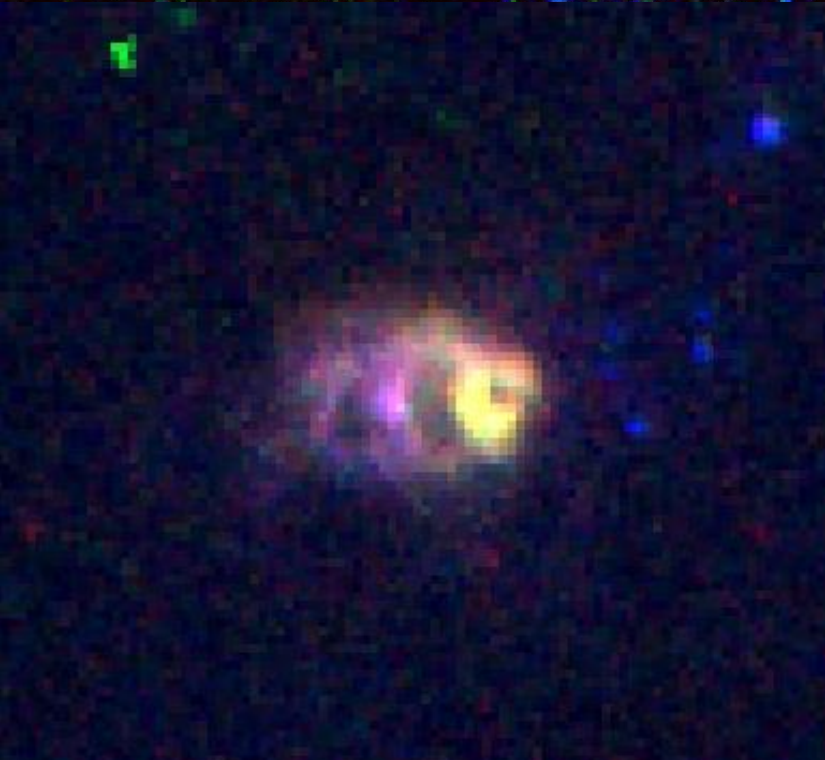
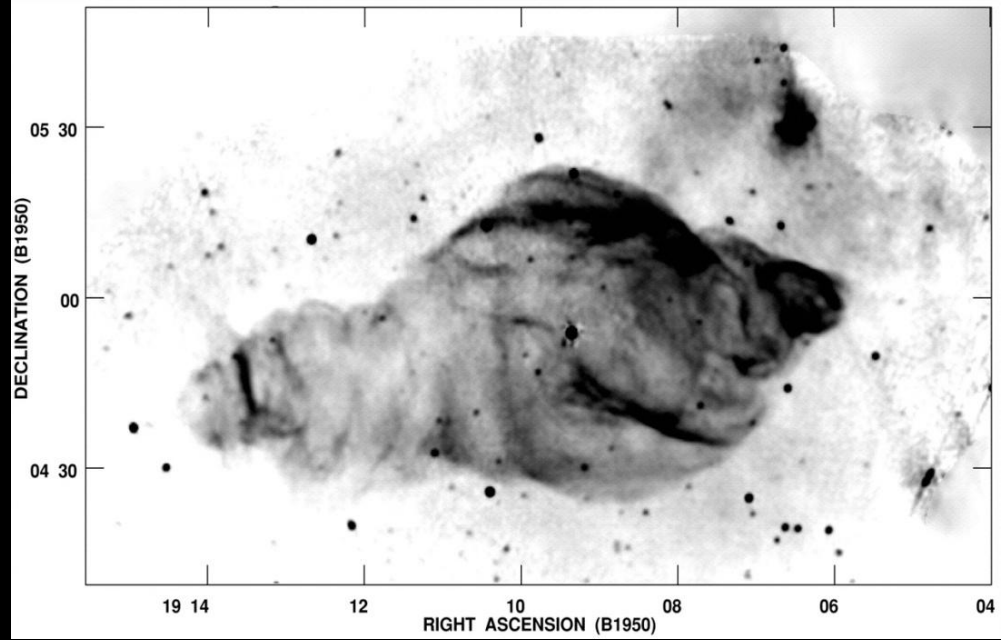
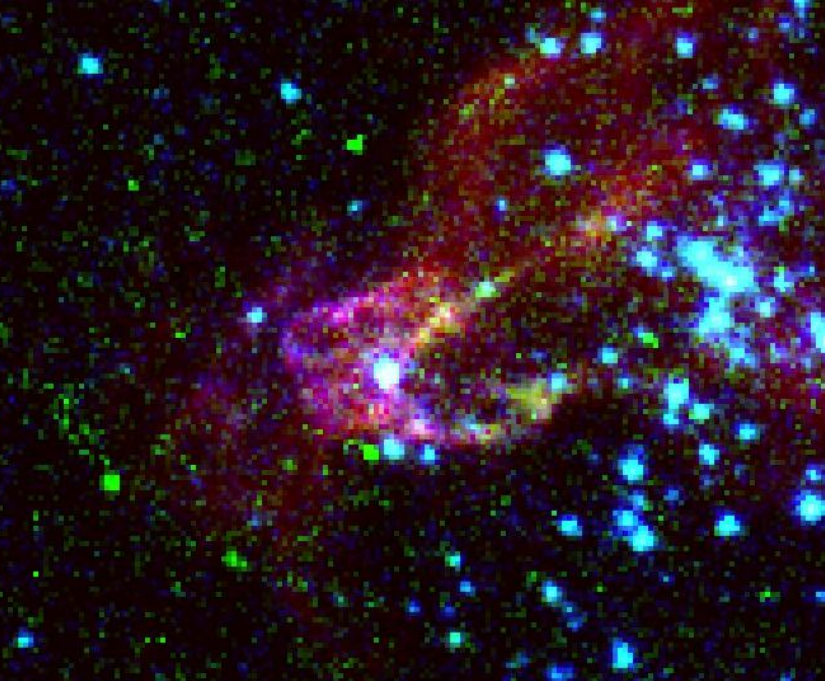


NGC 5204 X-1 (4.3 Mpc)

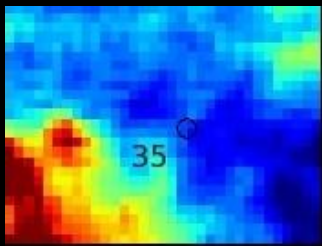


Holmberg II X-1 (3.05 Mpc)

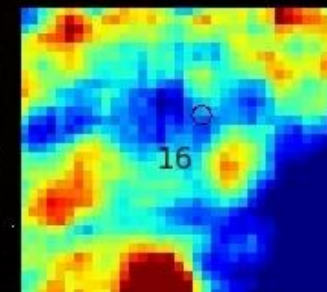
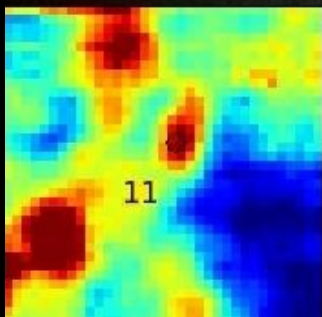
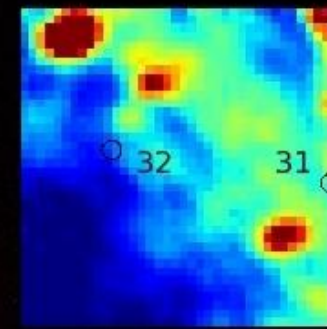
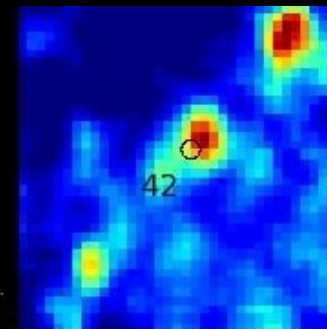
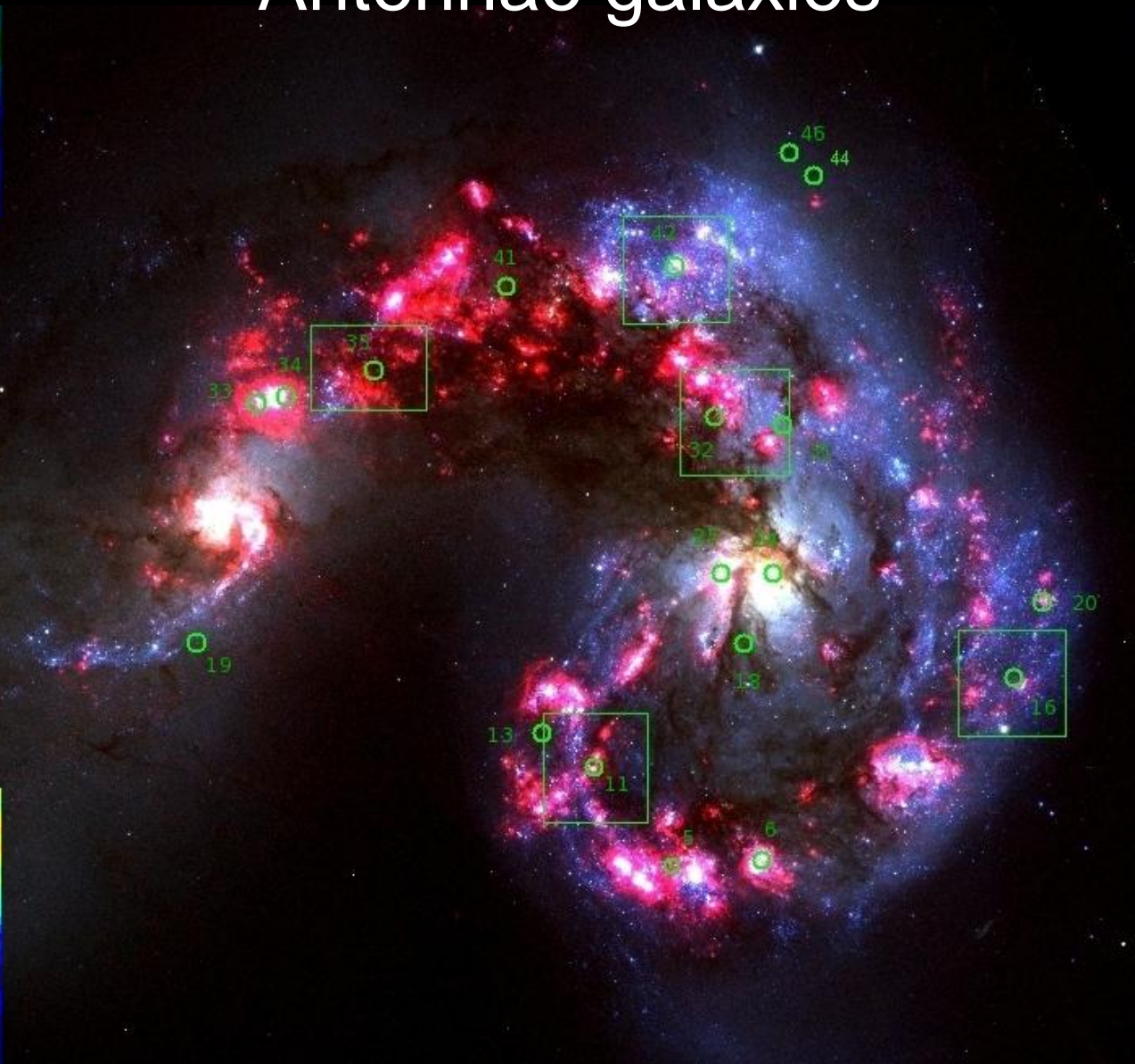




Antennae galaxies



E
N

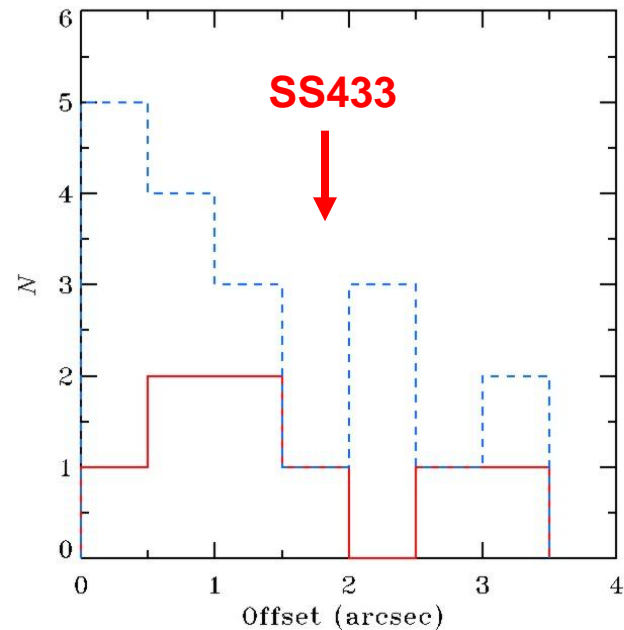
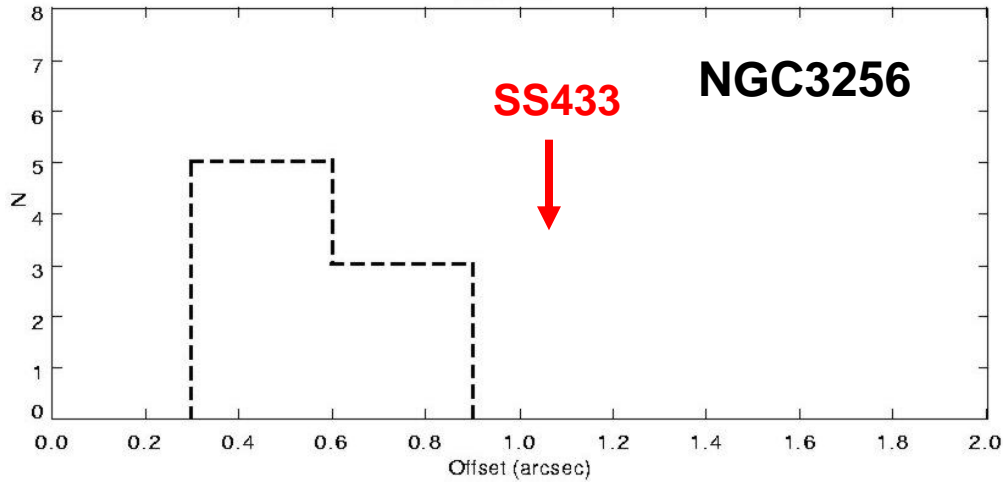


ULXs in Antennae



They are not in clusters

ULXs displacements in Antennae and NGC3256



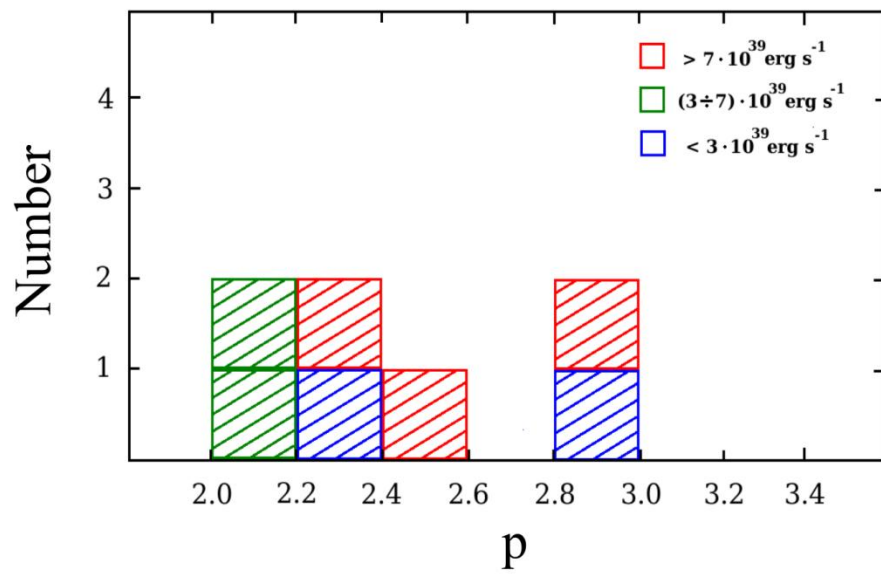
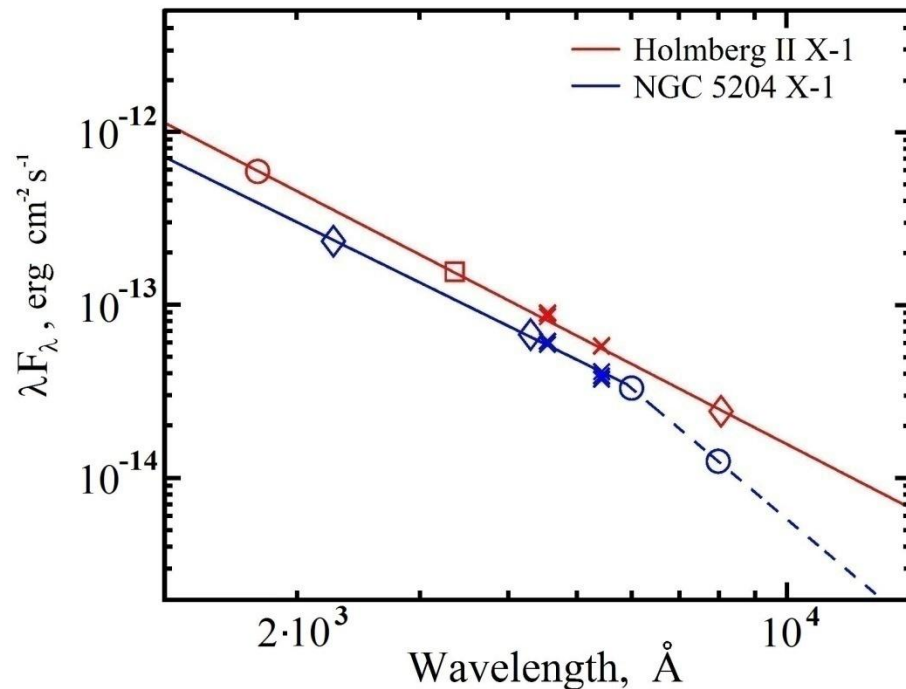
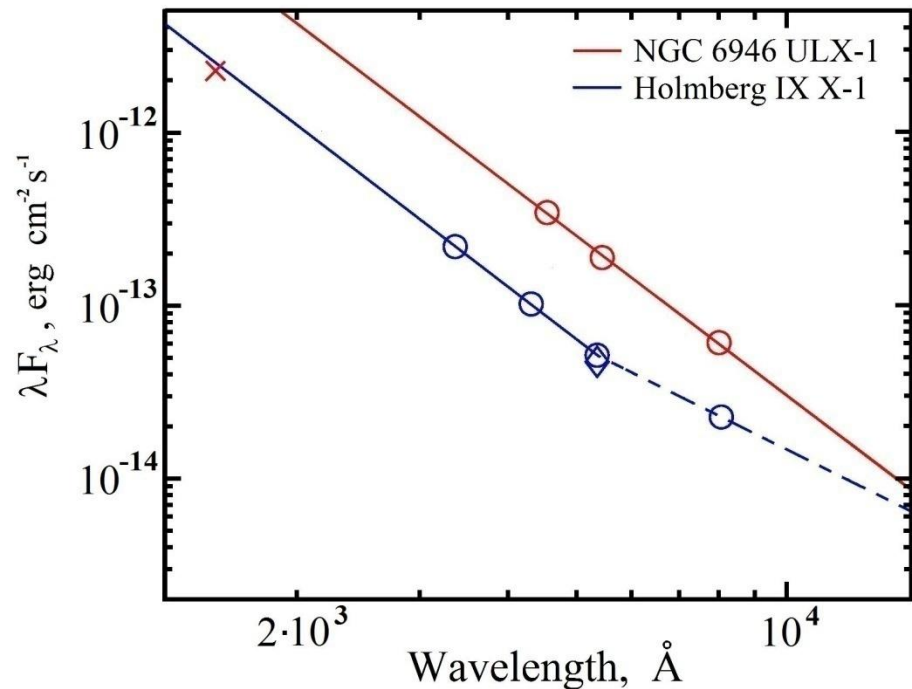
Antennae

sub-ULX + ULX

ULX

A distance of SS433 to nearest young clusters is about 200 pc in Galaxy

ULXs spectral energy distributions from the HST

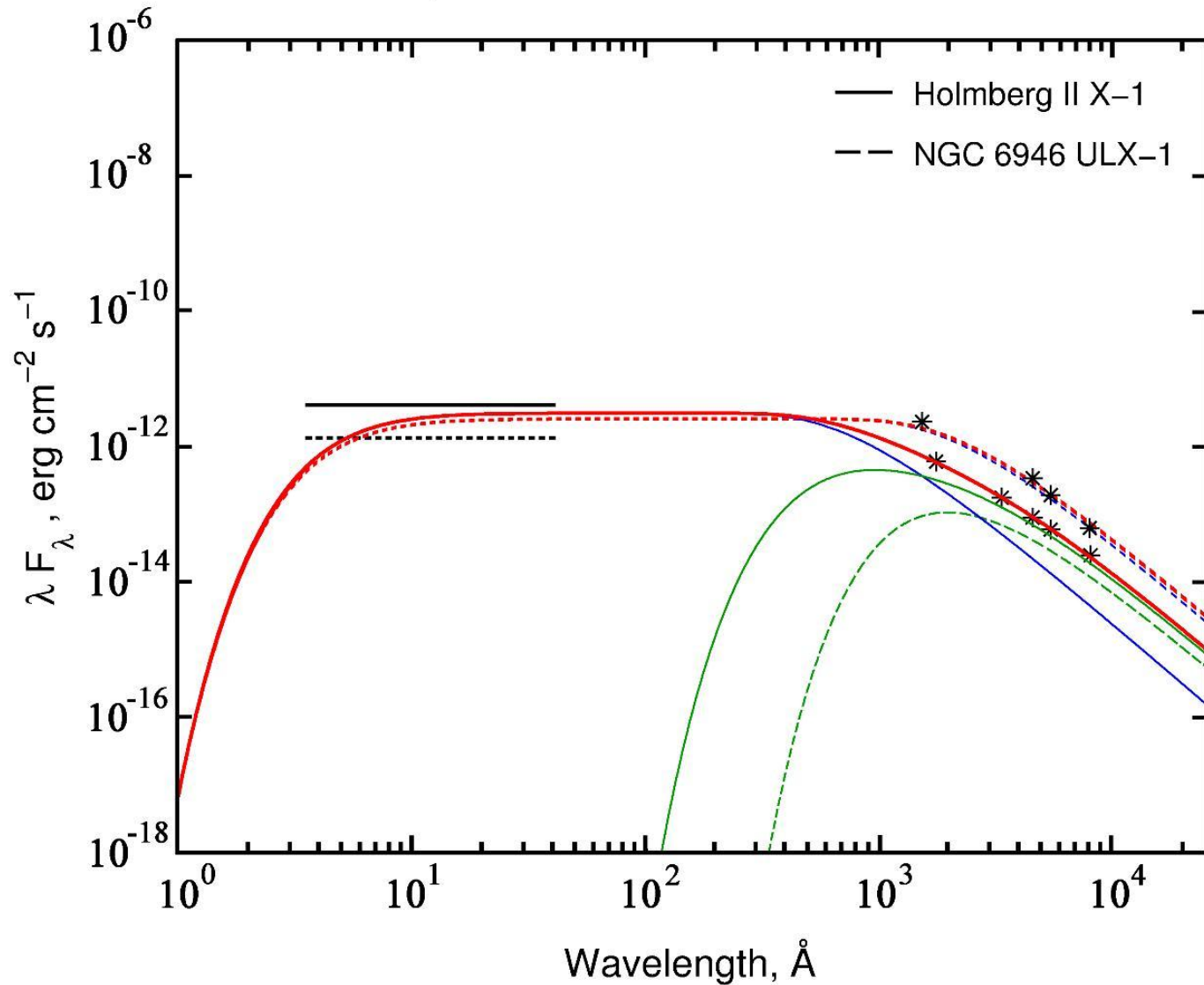


Spectral indices of ULXs

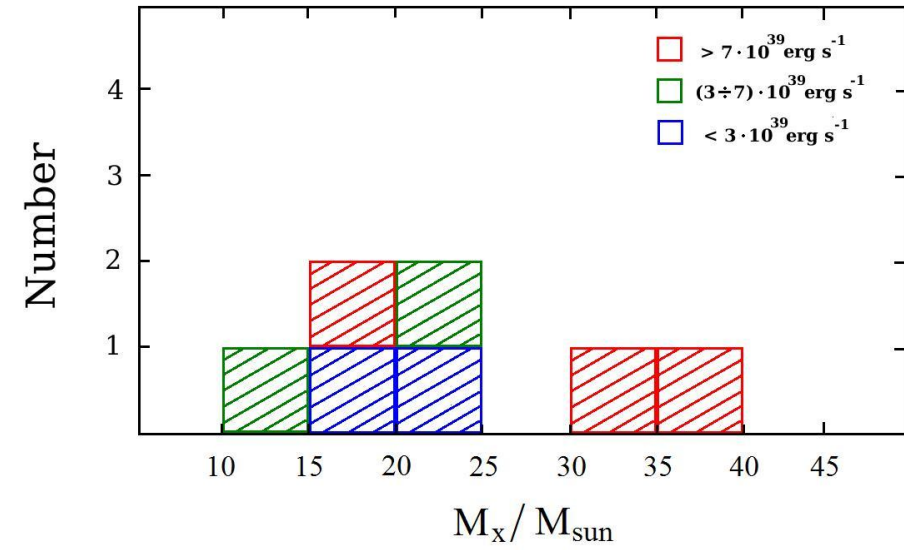
$$\lambda F_{\lambda} \propto \lambda^{-p}$$

λ

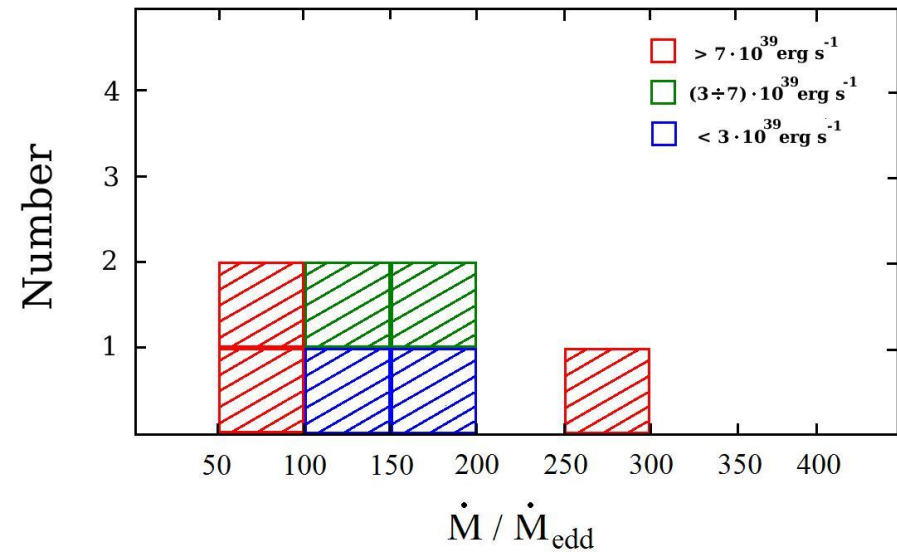
Observed and model spectra of ULXs (Shakura-Sunyaev model)



X-ray, UV and optical luminosities are about the same



Masses of black holes and
mass accretion rates in ULXs



Supercritical accretion onto supermassive black holes?

The fast growth of the SMBHs in the first billion years:

$3 \cdot 10^9 M_{SUN}$ for 800 Mys. Duty cycle $\sim 100\%$

$$t_S = \frac{M}{\dot{M}_{Edd}} = 3.2 \cdot 10^7 \text{ y} \quad M_{seedBH} \cdot 2^{\left(\frac{800My}{t_S}\right)} = 3 \cdot 10^9 M_{SUN}$$

$$M_{seedBH} \sim 100 M_{SUN}$$

$$\dot{m} = \frac{\dot{M}}{\dot{M}_{Edd}} > 1, \quad t_S \sim \frac{\dot{M}}{\dot{M}_{Edd}} \cdot \dot{m}^{-1} \sim \frac{M}{\dot{M}} \quad M_{seedBH} \sim \text{any}$$

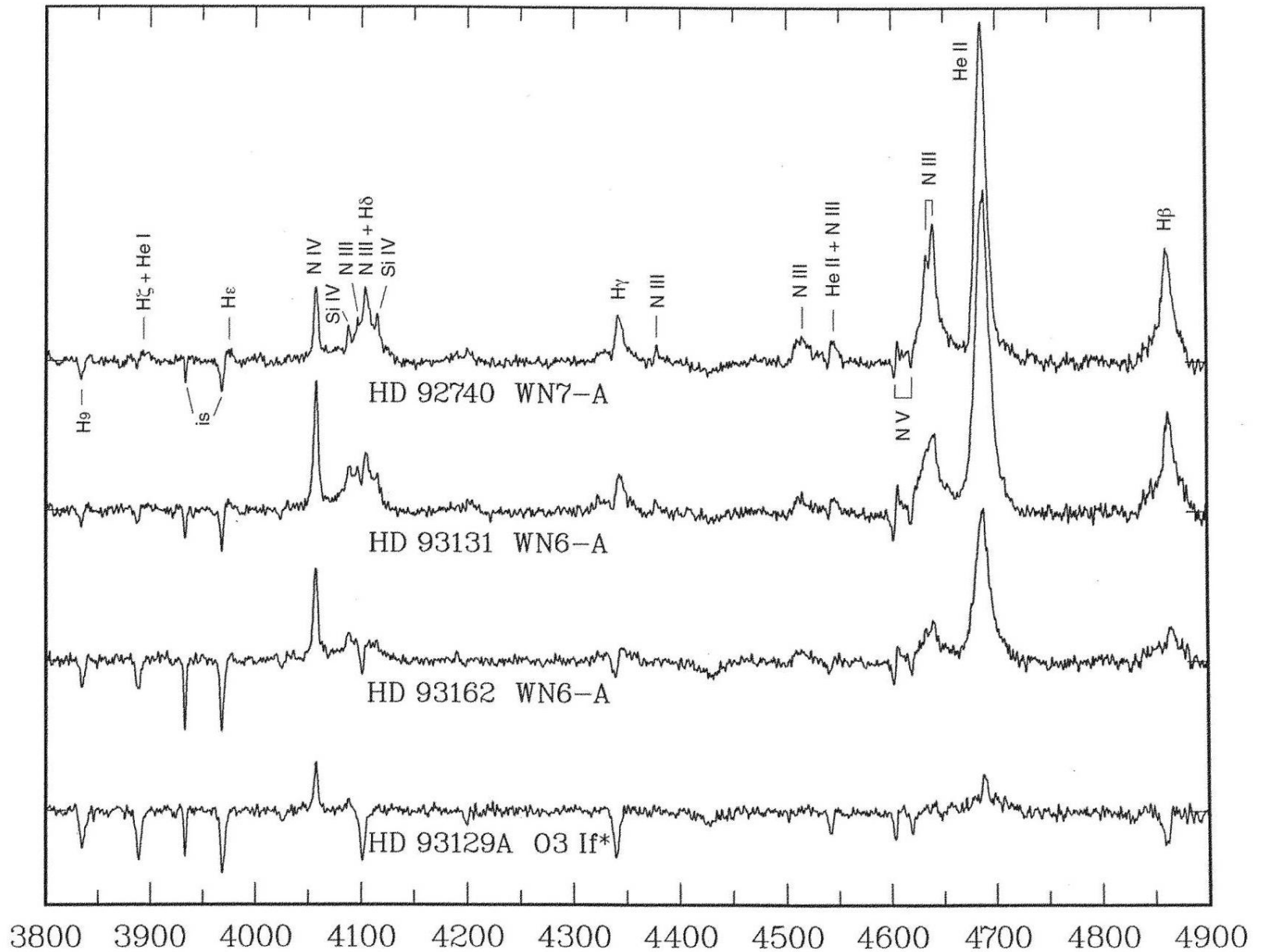
Episodes of supercritical accretion at nowadays. Duty cycle $< 1\%$.

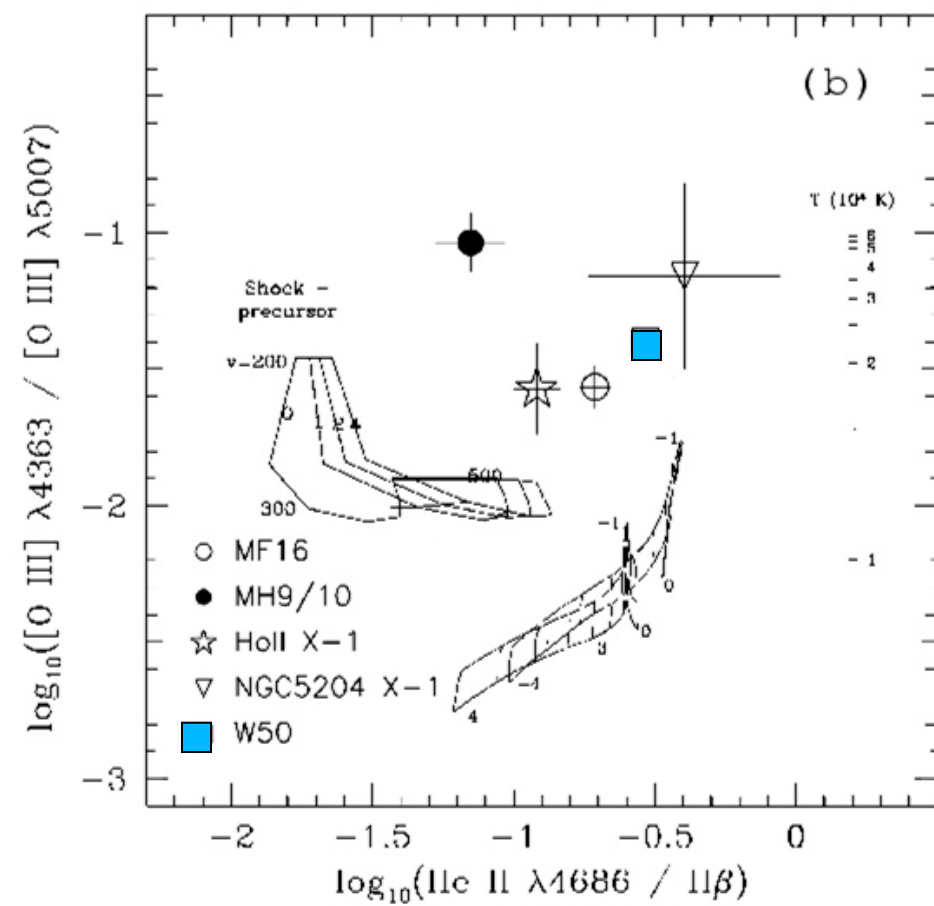
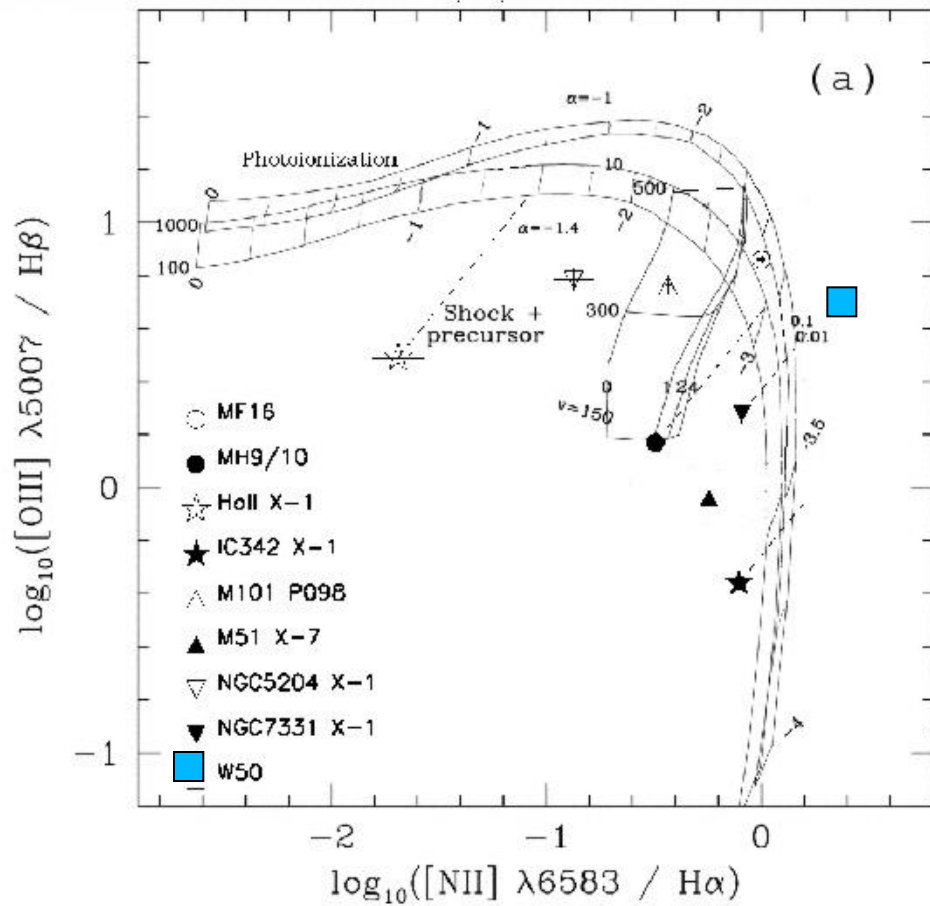
The obscured phase. IR-photospheres.

$$T_{ph} \leq 1000 \dot{m}_{300}^{-3/4} m_8^{-1/4} \text{ K}$$

Спасибо!

The OB Zoo: Walborn & Fitzpatrick, 2000

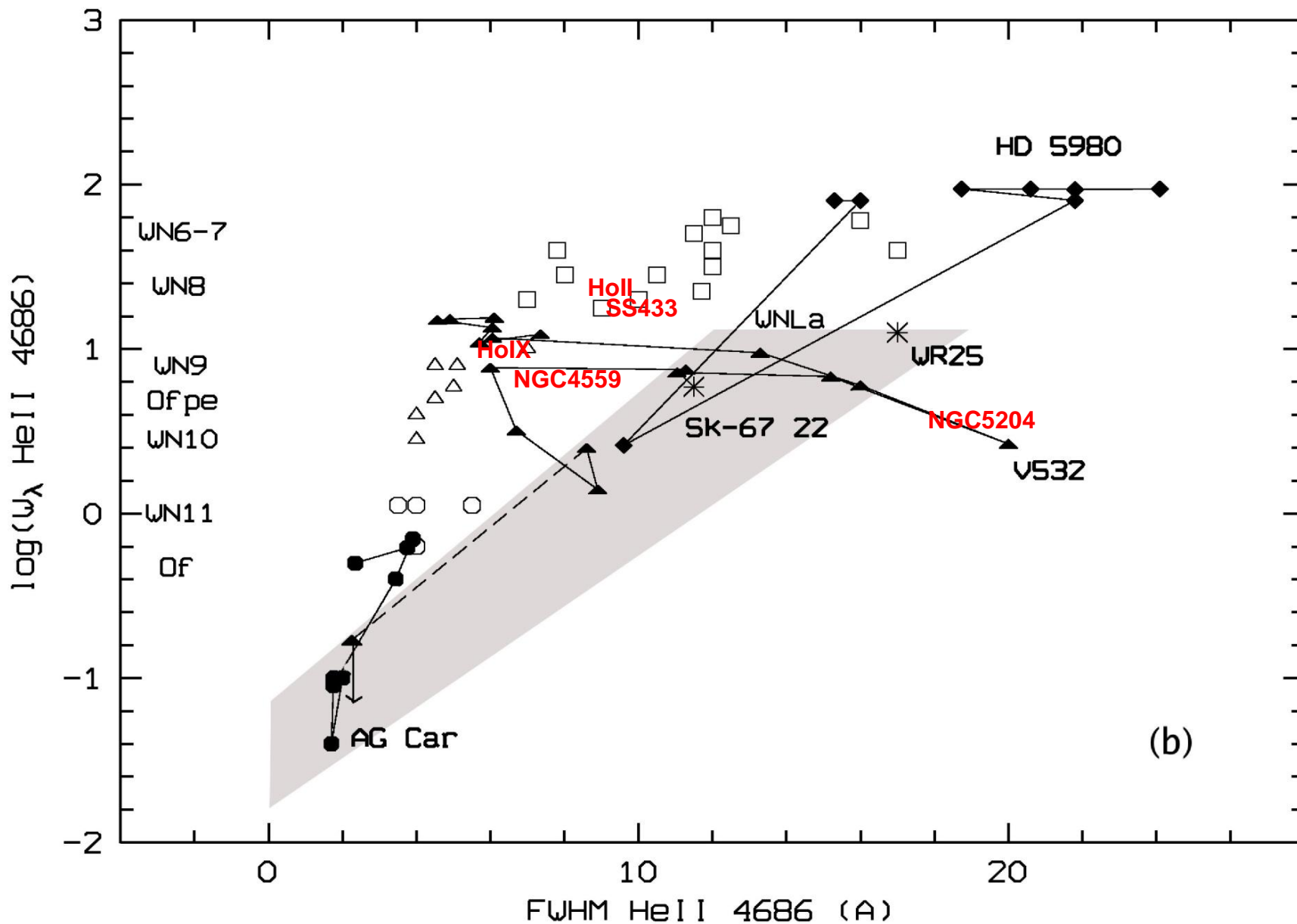




Туманности ULX и восточное волокно W50 на диагностических диаграммах

Классификационная диаграмма WN-звезд (Crowther & Smith, 1997)

Положение LBV-звезд AG Car, V532, HD5980 на этой диаграмме (Sholukhova et al., 2011)



Poutanen et al. (2007): calculations with wind and advection

$$\dot{m}_0 = 1000, \quad Q_0 = L_{\text{edd}}/4\pi r_{\text{in}}^3$$

